WEARABLE SURFACE ELECTROMYOGRAPHY (sEMG) TECHNOLOGIES WITH GRAPHENE TEXTILE ELECTRODES

by
ÖZBERK ÖZTÜRK

Submitted to the Graduate School of Engineering and Natural Sciences
in partial fulfilment of
the requirements for the degree of Master of Science

Sabancı University
September 2020

WEARABLE SURFACE ELECTROMYOGRAPHY (sEMG) TECHNOLOGIES WITH GRAPHENE TEXTILE ELECTRODES

Approved by:

Asst. Prof. Dr. MURAT KAYA YAPICI … 01/9/2020 ….
(Thesis Supervisor)

Prof. Dr. VOLKAN PATOĞLU..……..

Prof. Dr. BURAK GÜÇLÜ……..

Approval Date: September 1, 2020

ABSTRACT

WEARABLE SURFACE ELECTROMYOGRAPHY (sEMG) TECHNOLOGIES WITH GRAPHENE TEXTILE ELECTRODES

ÖZBERK ÖZTÜRK

Electronics Engineering M.Sc. THESIS, September 2020

Thesis Supervisor: Ast.Prof. Dr.Murat Kaya YAPICI

Keywords: surface electromyography (sEMG); EMG; textile; electrode; graphene; e-textile; wearable; flexible; health monitoring; IoT ; m-health

Ability to acquire, record, and process muscular biopotentials with wearable health trackers, diagnostic and/or assistive devices through the integration of soft, gel-free surface electrodes will enable seamless monitoring of muscle status in dynamic settings and can facilitate various applications. To this end, one of the fundamental limitations against the development of such systems is due to the drawbacks of clinical Ag/AgCl wet electrodes which have a gel layer that causes discomfort and can lead into skin irritation especially in wearable, portable applications with typically longer monitoring durations. The major objective of this thesis is to develop, explore and evaluate the application of novel and truly wearable graphene textile electrodes specifically in surface electromyography (sEMG) applications. Benchmarking of the textile electrodes with respect to clinical electrodes was performed in terms of their skin electrode impedance (SEI) values and signal-to-noise ratios (SNR) acquired through static experiments. SEI values of textile electrodes were found to be well within the acceptable range and comparison of SNR values showed that graphene textile performance in static settings swings between 65% and 90% level of clinical signal quality. Custom-designed wearable platforms consist of muscle specific elastic bands with integrated graphene electrodes and battery-powered, small footprint hardware that can stream data wirelessly over Bluetooth. Feasibility of the developed wearables were shown with two different applications in dynamic conditions where a calf band was designed and used for activity tracking, and an arm band was developed for localized muscle fatigue assessment. The holistic system design

concept presented here that is inclusive of fundamental material aspects up to the implementation of high-level user interface will be valuable for the development of wearable EMG platforms.

ÖZET

GRAFEN TEKSTIL ELEKTROTLARLA GIYILEBILIR YÜZEY ELEKTROMYOGRAFI (sEMG) TEKNOLOJILERI

ÖZBERK ÖZTÜRK

ELEKTRONİK MÜHENDİSLİĞİ YÜKSEK LİSANS TEZİ, EYLÜL 2020

Tez Danışmanı: Ast.Prof. Dr.Murat Kaya YAPICI

Anahtar Kelimeler: tekstil elektrot, EMG, giyilebilir elektronik, adım-ölçer, kas yorgunluğu

Giyilebilir cihazlara yüzey elektrotlarının eklenerek EMG ölçüm işlevinin kazandırılması, dinamik koşullarda kas statüsü takibine izin verdiğinden birbirinden farklı çok sayıda uygulamanın önünü açma potansiyeline sahiptir. Bu tip sistemlerin önündeki teknolojik problemlerden birisi, uzun süreli ölçümler için uygun olmayan klinik ıslak elektrotların problemlerini çözmek adına kuru yüzey elektrotlarının geliştirilmesidir. Bu bağlamda, sunulan çalışmanın ana amacını geliştirilen grafen tekstil elektrotların karakterizasyonu ve giyilebilir uygulamalardaki performanslarının değerlendirilmesi oluşturmaktadır. Tekstil elektrotların klinik elektrotlarla kıyaslanması, cilt-elektrot empedans (SEI) değerleri ve statik deneyler yoluyla elde edilen sinyal-gürültü oranlarıyla (SNR) yapıldı. Tekstil elektrotlarının SEI değerlerinin kabul edilebilir aralıkta bulunduğu ve SNR değerlerinin karşılaştırılmasıyla da, statik ortamlarda grafen tekstil ile elde edilen performansın klinik sinyal kalitesinin % 65 ile % 90 arasında değiştiğini göstermiştir. Özel olarak tasarlanmış giyilebilir platformlar, Bluetooth aracılığıyla kablosuz olarak veri akışı sağlayabilen, entegre grafen elektrotlar ve pille çalışan, az yer kaplayan donanım içeren ölçüm alınan kasa özgü elastik bantlardan oluşmaktadır. Bu giyilebilir ürünlerin uygunluğu iki farklı uygulama ile gösterilirken, bir bacak bandıyla aktivite takibi bir kol bandıyla da lokalize kas yorgunluğu değerlendirmesi yapılmıştır. Burada verilen sistem konsepti, en temel iletken tekstil üretiminden son seviyedeki kullanıcı arayüzüne kadar izlediği yaklaşımla, giyilebilir EMG platformlarının geliştirilmesi için katkı sağlamaktadır.

ACKNOWLEDGEMENTS

This section of the thesis will be more of a thank you card than digging into the details of contributions that I had received. However, I should start by stating that the primary source of assistance to this work came, not surprisingly, from my advisor Asst. Prof. Dr. Murat Kaya Yapici. I met with this topic through him, and throughout the project, he guided me, which I needed a lot in times of uncertainty. Under his supervision, I understood the academy and what does it mean to be a researcher.

Then, I need to talk about Ata Golparvar and Gizem Acar. In addition to being dear friends to me, they were fellow researchers whom I worked together on graphene textile electrodes. Thanks to Gizem's efforts to perfect the conductive textile fabrication process, we had workable electrodes for our designs. On the other hand, Ata designed the acquisition systems that we had used, which were adaptable for different biosignal acquisition scenarios. My job became relatively comfortable with their contributions, and I focused more on application sides.

Thesis writing is not an easy task by itself; I also experienced that together with Melih Can Taşdelen, who was passing through the same process. It was not an easy time for both of us, and without his companionship, it would be harder to bear for me. I won't forget the times that we spent together in the lounge.

I feel lucky to say that for my research group, I was surrounded by people whom I was able to call friends. Other than the four people mentioned above, I would like to thank Osman Şahin, Sercan Tanyeli, Farid Sayar Irani, Tuğçe Delipınar, Ekin Özek, Rayan Bajwa, and Heba Saleh. They all provided valuable and honest support for me whenever possible.

Finally, I'm sending my hugs to my sister and my parents from here. Their existence makes me a stronger person than I am, and all the things that I have accomplished are thanks to them.

To the days left behind...
Geride kalan günlere...

LIST OF ABBREVIATIONS

TABLE OF CONTENTS

LIST OF TABLES

LIST OF FIGURES

I. INTRODUCTION

The wearable electronics market has doubled from 2014 to 2019 and transformed to a $50bn worth industry [1]. This immense growth has been fueled by the miniaturization trend of microelectronics, advancements in flexible electronics, and the internet of things (IoT). The market growth ignited by the fitness tracking devices was followed by the introduction of smartwatches, smart goggles, and especially in the last two years with "smart" headphones, otherwise referred to as hearables [2]. It seems that the above-mentioned devices have not fully reached their market potential, and their growth will continue while new wearables could be expected to emerge in the consumer market like smart garments.

Smart garments, garments with sensing and actuation capabilities, are showing themselves as next in the line. However, it was still surprising news when two of Dutch short track speed skaters for the 2018 winter Olympics were using SmartSuit created by Samsung in their training. It allowed them to track their postures in real time with great accuracy and provided feedback for gaining optimal muscle memories in their movements [3]. In the Olympics, athletes trained with SmartSuit returned with gold and silver metals with supporting the idea that smart garments could be used in practical situations such as elite athlete training. Replacement of traditional garments with wearables opens the possibility to situate sensors/actuators nearly anywhere on the skin surface. It could also enable a plethora of applications with physiological information directly from the body. Although existing wearables, especially smartwatches, can provide temperature sensing and pulse monitoring capabilities, smart garments can be integrated with surface electrodes and corresponding electronics to sense bioelectric potentials such as electrocardiogram (ECG), electroencephalogram (EEG) and electromyogram (EMG). It is plausible to imagine a future where people cloth with portable, omnipresent biosignal acquisition units. Continuous acquisition of biosignals could enable a plethora of applications that were not relevant in static lab settings and pave the way for the flood of new research on this dynamic paradigm. The possibility of EMG acquisition in real-world settings is especially appealing since it allows muscle status monitoring in relevant

scenarios where subject movement is not constrained.

Electric potentials produced by skeletal muscles could be either picked up by needle electrodes inserted nearby the muscle site where the technique is called intramuscular electromyography (iEMG) or with surface electrodes attached to the skin surface hence surface electromyography (sEMG) [4]. iEMG can provide specific information about the muscle up to single motor unit activation. In contrast, sEMG provides a combined representation of activated motor units subjected to spatial and frequency domain filtering due to tissues in between and electrode size and configuration [5]. The loss on locality and fidelity of the signal is a compromise against the ease of application and non-invasiveness of sEMG recordings. It may be argued that intramuscular and surface EMG complement each other; iEMG is used more for diagnostic purposes. In contrast, surface EMG is used for different applications in various fields ranging from ergonomics, prosthetics, human-computer interaction (HCI)to sport sciences and rehabilitation [6, 7, 8, 9]. For example, sEMG information has been used as a control signal in a prosthetic arm [7], an indicator of the muscle status, which is useful to improve athlete performance [10] or rehabilitation of a muscle group in physiotherapy [11]. It can be used in gait analysis to improve the ergonomics of walking or running [12], and it can provide biofeedback for sleep bruxism treatment [13].

Electrodes usually preferred in sEMG data acquisition are pre-gelled, disposable silver/silver chloride (Ag/AgCl) electrodes that are fixed to the skin on the muscle of interest with adhesive tape. Their characteristics are relatively close to the non-polarizable electrodes, making them less susceptible to relative movements between electrode and skin. The electrolyte gel also helps create a stable interface to ensure a high signal-to-noise ratio (SNR) in the acquired signal [14]. However, when long term and out of laboratory recordings are desired, for smart garments, Ag/AgCl electrodes seem to carry some drawbacks including: (1) skin irritation caused by the gel and adhesive backing [15], (2) drop in the signal quality with drying out of the gel, and (3) the need for someone with enough physiological knowledge to properly place the electrodes on the desired muscle. The earlier two of these problems are attributed to the existence of the gel, and a straightforward answer to them is simply to use gel-less dry electrodes. Unfortunately, implementation is not as straightforward as it might suggest because the gel has valuable objectives such as providing skin contact over hair, preserving the skin contact against small movements induced on the electrode, and keeping the skin itself conductive [4]. This fundamental trade made the dry electrode research an active research topic; in fact, search for dry electrodes with optimal performance still continuous. The last drawback of the wet electrodes, on the other hand, can be solved with the utilization of smart garments where all the

electrodes can be placed on predetermined locations, which frees the user from the assistance of a physiologist. Thus, using dry surface electrodes on smart garment design intuitively appears as progress for continuous monitoring. Among the dry electrodes, one specific electrode type is a natural candidate: textile electrodes or textrodes. They offer seamless integration with the garment and promise great comfort due to their softness and breathability [16]. However, the above advantages must need to be obtained with minimum compromise on signal quality since the fidelity of the signal picked up at the analog front-end affects all the subsequent processing, and it is nearly impossible to improve signal quality afterward [17]. Therefore, the textile electrode design providing high fidelity and a high signal-to-noise ratio recording is an important part of a wearable bio-signal monitoring paradigm.

Researchers have devised different ways to bestow conductivity on ordinary fabrics. The main approach is usually to find a method to integrate conductive materials with fibers and yarns firmly. Frequently used conductive materials can be classified as metals, conductive polymers, and carbon allotropes such as carbon nanotubes and graphene [18]. Integration of these materials can vary from common fabric manufacturing techniques (e.g. knitting, weaving) [19], decoration techniques (e.g. embroidery, printing) [20, 21], to electroplating [22] and chemical polymerization [23]. One of the obstacles ahead of low-cost production of conductive textiles and textile electrodes is the adaptability of conductive textile fabrication techniques to existing industrial textile manufacturing and finishing processes. Most of the preceding techniques ask for specific equipment, facilities, or process steps that limit fabrication's scalability to larger quantities. On the other hand, our group followed a scalable dip-dry-reduce fabrication technique to coat textile surfaces with graphene and previously pioneered the development of graphene-coated conductive textiles as electrodes for monitoring cardiac and ocular potentials [24, 15]. Graphene is an exciting choice for its remarkable electrical, mechanical, and thermal properties. The scalability of the graphene textile synthesis process allows the imparting electrical conductivity to large sizes of ordinary textiles (such as nylon, cotton, wool) while preserving their texture and softness.

In this work, graphene electrodes and wearables integrated with these electrodes for sEMG recording is presented. Comparisons of graphene electrodes with clinical electrodes revealed a desirable level of performance correlation. Furthermore, the usability of textile electrodes in dynamic applications was showed with implementing muscle-specific wearable bands for peroneus longus and biceps brachii muscles. Designed "calf band" for peroneus longus was used to create a pedometer functionality, whereas "armband" designed for biceps brachii was used for extracting fatigue indi-

cators. Obtained results showed a good correlation with a commercial step-counter and suggest developed systems could be used to construct standalone pedometers or combined with accelerometers to create highly accurate pedometers. On the other hand, signals that were harvested with armband provided enough fidelity for muscle fatigue detection. These represented a proof-of-concept for bioelectric potential acquisition with smart garments.

The outline of the thesis is presented as follows. After the general information is given in this chapter, the next two aims to give background information on EMG and textile electrodes, respectively. The fourth chapter will cover the preparation of the graphene wearables, starting with the conductive textile fabrication, electrode fabrication, and characterization. Afterward, it will be concluded with performance comparisons with commercial Ag/AgCl in static conditions. Applications tried with wearable bands (step counter and fatigue indicator) will be explained in the fifth chapter—the last chapter addresses long term usability concerns with the washability and biocompatibility of the fabricated electrodes.

II. ORIGINS OF EMG

Today's cutting edge robotic technology is at an extraordinary level where it is possible to see a humanoid robot to do a backflip as Atlas from Boston Dynamics(MA, USA). This level, of course, requires the use of state of the art hardware and control system. Human locomotion and manipulation capability are so fascinating that it's always intriguing to see robots capable of doing similar actions. In the human body, skeletal muscles can be regarded as the actuators during the neuromuscular system as the controller. They enable a sprinter to run 100 meters under 10 seconds, allow a piano player to express subtle emotions under the fingertips, or throw a rock to a lake. It is possible to gain insight into these mechanisms with acquiring biopotentials produced by skeletal muscles, called electromyography (EMG). As it is stated by Merletti and Parker (2004), "provides a window on the motor as well as on its controller" [4]. Although muscle activity can be tracked with sensing the magnetic fields created by the ionic currents by magnetomyography [25] or with sensing mechanical oscillations produced by muscle fibers by mechanomyography [26], they are less studied and utilized compared to EMG.

Animal electricity fascinated the curious minds of society for some time. Historical investigation of the relationship between muscle activation and electricity could be originated with Francesco Redi's work with electric ray fish dating back to 1666, where he observed specialized muscles of the ray fish are capable of producing electricity [27]. Then, Luigi Galvani published an observation at 1792 in which it's shown that electricity could start contractions of muscles [28]. The reverse effect of this, where voluntary contraction causes the generation of electric potential discovered nearly sixty years later, in 1849, by Dubois-Raymond. Name the father of the term "Electomyograpghy" was Marey, who also performed the first EMG acquisition in 1890 [29]. The first modern recording could be dated back to 1922 when Gasser and Erlanger utilized an oscilloscope to record the phenomena. Advances in the recording electronics and electrodes improved the quality of the recorded signals steadily. Surface electromyography started to be used as a clinical tool in the 1960s, and with the availability of recording cables in the 1980s, features in the microvolt

level could be distinguished [29]. For the clinical recordings, sEMG has been used for superficial skeletal muscles, whereas intramuscular EMG has been used for deeper muscles.

This chapter aims to lay the background on wearable surface EMG applications, which will be recalled back on chapter four with going over the physiology of muscle biopotentials and acquisition systems developed on them.

1 Physiology of EMG

As the signals generated by skeletal muscles, EMG could directly be considered as carrying information on control of movement by the brain. However, to be able to extract this information, it is required to understand the neuromuscular system. At least on a higher level where torque exertions by muscle fibers and their activation signals starting from the related brain cortex.

The smallest functional unit of the neuromuscular system is called motor unit (MU). It comprises an alpha motoneuron and muscle fibers innervated by the motoneuron [4]. Propagating action potentials in these fibers activates the contractile proteins and results in a twitch of related fibers. According to the function of the specific muscle, the number of MUs in a muscle and force-generating capacity of individual MUs change. Small hand muscles, for example, have around a hundred MUs, whereas large limb muscles generally have around a thousand [30]. Moreover, in the same muscle, the force exerted by a single MU can vary a hundredfold [31].

Control of motor units through their alpha motoneurons happens in the central nervous system in top-down order. After the motor programming in the brain's related areas, inputs from these areas, together with ones coming from the cerebellum and basal ganglia, converge in the primary motor cortex. Primary motor cortex outputs to the motoneurons and interneurons of the spinal cord, and then with the connection between the corticospinal tract and alpha motoneurons muscle control occurs (Fig.2.1) [4].

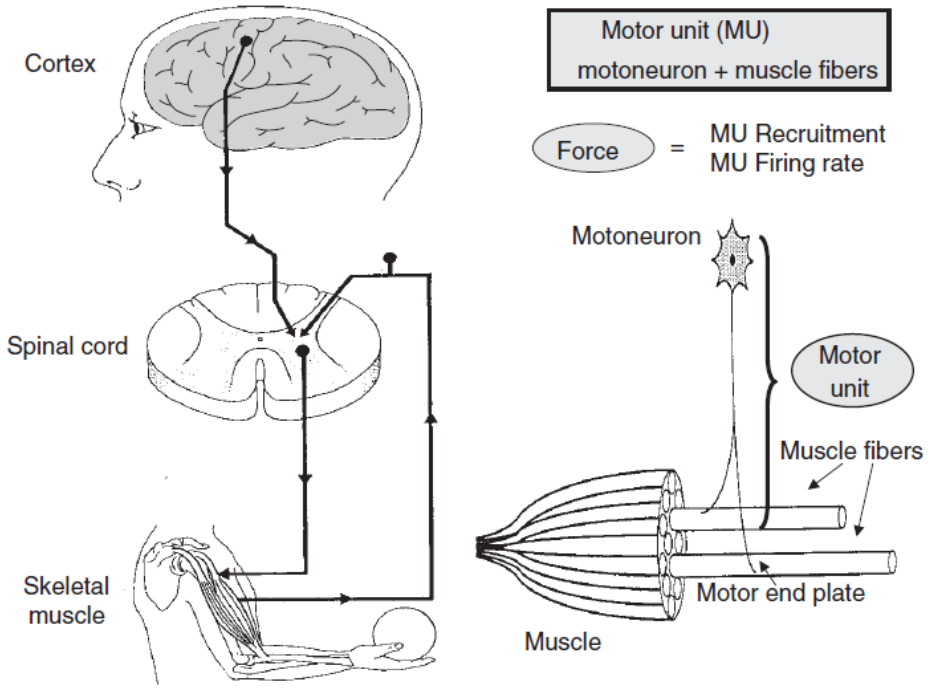

Figure 2.1 Hierarchical structure of central nervous system as motor unit activation occurs [4]

Bioelectric potentials occur due to the contraction of muscle fibers, where depolarizing and repolarizing zones act as the signal sources. Signals can be recorded either with intramuscular needle electrodes or with the surface electrodes, where acquired signal quality is lower in the latter one because of the greater amount of tissue present, which has a spatial and temporal low pass filter effect on the original signal [27]. However, except for the motor unit action potential monitoring [32], surface EMG(sEMG) is widely preferred over intramuscular EMG due to its non-invasive nature and convenience. It is also natural to use sEMG in wearable systems since repeatable and unassisted user experience is always preferred.

2 sEMG Acquisition

Twenty years ago European Union initiated a concerted action for standardization of sEMG recording parameters (electrode placement, size, inter-electrode distance, front-end amplifier) called SENIAM (Surface Electromyography for the Non-Invasive Assessment of Muscles) which was at that time showed essential differences from one researcher to another and data exchange between different groups were nearly im-

possible [33]. Although two decades passed over this initiation and new techniques such as multichannel EMG emerged and requires further standardization, recommendations over single-channel EMG acquisition are still valid and used.

2.1 Electrodes

Biopotential electrodes can be thought of as the interface between the in-body ionic currents and electron currents of the recording electronics. Therefore, electrode performance has a direct effect on the acquired signal quality since the signal picked up at the analog front-end affects all the consecutive processing, and it is nearly impossible to improve it afterward [17].

The effect of the electrode can be better visualized by representing the electrical signal path with a simple equivalent circuit. Fig.2.2(a) illustrates signals emanated from the muscle fiber passes the tissues, which effectively working as volume conductors and reaches to the skin surface, where it goes through complex electrode-skin interface Z_e and picked up by the input impedance of the amplifier Z_i.

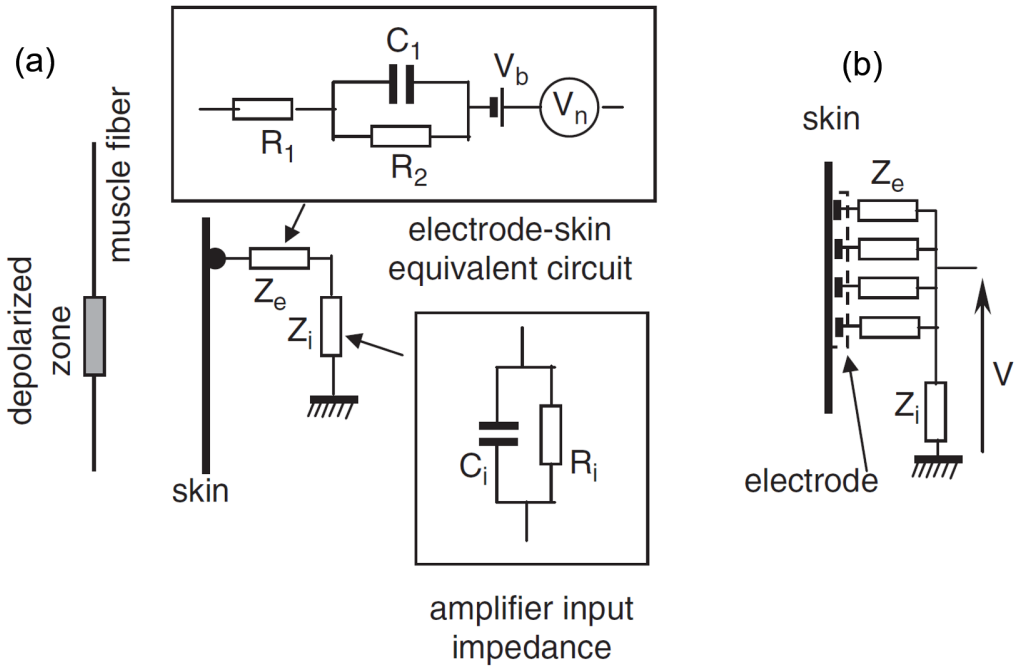

Figure 2.2 (a)Electrical representation of biopotential path (b) Due to the fact that electrode has finite area, it does not act as a point electrode but rather as a point electrodes connected in parallel [4]

As shown in Fig.2.2(b), real sEMG electrodes are not "point" electrodes due to

their finite area; however, point electrode approximation still can be used to express the whole structure with assuming every contact point between electrode and skin represents a point electrode. Thus, the finite electrode can be represented with a parallel combination of these point electrodes. This implies that recorded voltage will be the average of potentials carried by individual contact points, an average of potentials occurring underneath the electrode surface [34]. Surface electrodes, therefore, works as a spatial smoothing filter. It is also evident from here how larger electrode area results in smaller skin-electrode impedance.

There are some properties that the acquisition system must meet for a quality recording (Fig.2.3). For example, starting with the electrode, skin-electrode impedance should be less than 0.5 MΩs to avoid a significant voltage drop when combined with a reasonably high amplifier input impedance of 100 MΩ. Analog front end should provide a common-mode rejection ratio (CMRR) around 100 dB at power line frequency and its harmonics also should have AC coupling for DC offset removal and have a passband of for surface EMG signal of 20-500 Hz. Analog to Digital Converter is also expected to provide a high resolution with the wider availability of delta-sigma converters compared to past really high-resolution values can be acquired.

Further details on electrodes and the analog front end design will be provided on the following chapters through details of textile electrodes and developed acquisition system.

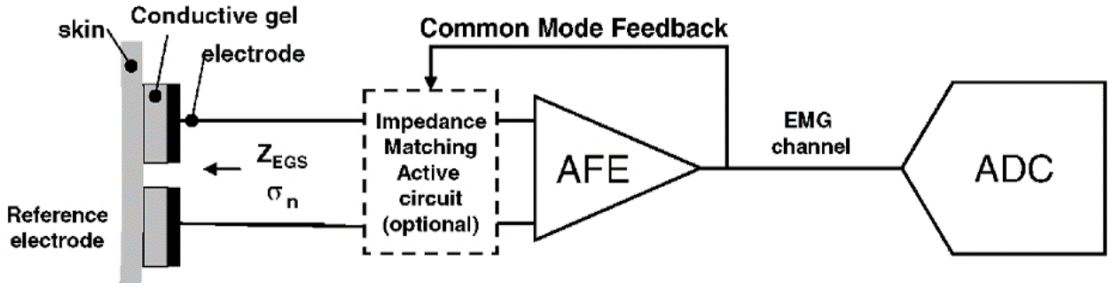

Figure 2.3 A general look on an analog front-end and analog to digital converter requirements and features[5]

III. BACKGROUND ON TEXTILE ELECTRODES

For thousands of years, textiles have been an integral part of our daily life for clothing and decoration. As the research on smart garments tries to add functionality to plain textile structure with sensors and actuators, preserving the wearable aspect of the textiles is important. It is, therefore, instinctive to use functional textiles such as textile electrodes to preserve the texture of the garments. Possibility of using textile electrodes in various scenarios are previously investigated in the literature such as electrochemical capacitors [35], solar cells [36] and neuromuscular stimulation [37]. This section, on the other hand, will have a closer look at biosignal acquisition electrodes.

1 Textile Electrode Fabrication

Textile electrodes for biopotential sensing are thought of as a specific application of conductive textiles. It makes sense, therefore, to look on the conductive textile fabrication step in more detail since it is one of the most important determinants of the cost and durability of the fabricated electrode.

Fabrication of e-textiles essentially relies on the stable integration of conductive materials with fabrics and fibers. Commonly used conductive materials include metals, conductive polymers, and carbon allotropes (i.e., graphene and carbon nanotubes). These materials can be used either with mainstream fabric manufacturing/decoration approaches (e.g. knitting, weaving, embroidery) [38], or can be applied onto finished textiles with various techniques like electroplating [22, 39] physical vapor deposition (PVD) [40, 41] chemical polymerization [23], dip-coating [42], and printing methods [43] to coat the surface of the textile (Fig.3.1) [44].

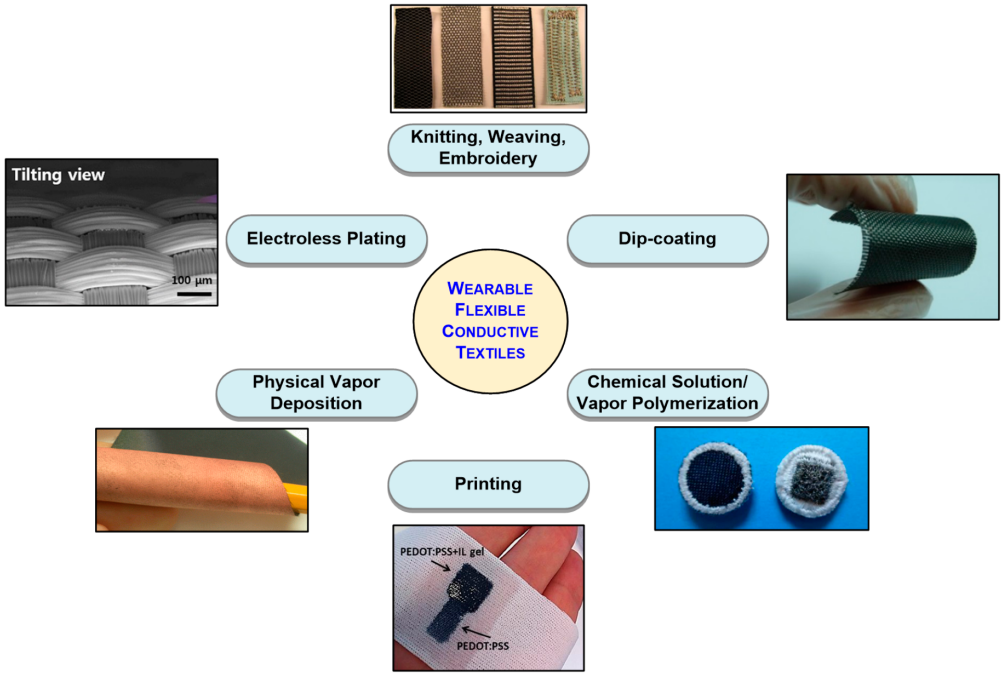

Figure 3.1 Main methods used in electroconductive textile fabrication. [42, 43, 45, 46, 47]

Regarding the cost of the conductive textiles, the raw materials, and equipment, together with the fabrication's scalability, all, of course, adds up for the final price.

Another concern is about the durability of the conductive textiles, which is related to the ability to preserve its conductivity after repeated use. Regarding the wearable biopotential applications, it is also desired to wash the electrodes together with structural textile parts. Therefore, conductive textiles should also have a wash resistance.

2 Performance Characteristic Analysis

In biopotential recordings, skin-electrode contact impedance is critical as it directly acts the received signal at the amplifier output. The effect is analogous to the filtering of the actual biopotentials emanating from the body [48]. If we assume the skin-electrode contact impedance of both electrodes to be equal

$$Z_{1(w)} = Z_{2(w)}$$

and name it as $Z(w)$, and similarly, the amplifier input impedance is seen by each electrode to be the same

$$R_{i1} = R_{i2}$$

, then the transfer function of the system H(s) can be expressed as the ratio of the amplifier output V_o to the biosignals V_1 and V_2 emanating from the body, as shown in Fig.3.2 [18].

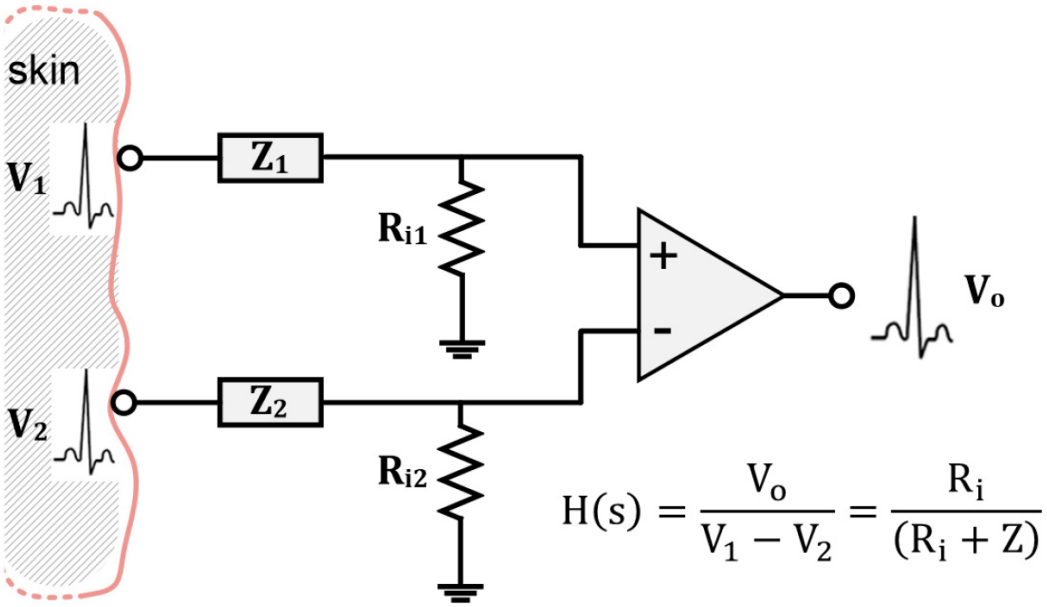

Figure 3.2 Schematic representation of the path of biopotential signals starting from the skin surface until acquisition and display at the circuit output [44]

An electrode-electrolyte interface can be modeled by a parallel RC network [49]. However, the skin is more complex; understanding skin-electrode impedance and its frequency-dependent characteristics requires investigation of the skin itself, consisting of three main layers: epidermis, dermis, and hypodermis or subcutaneous tissue [44].

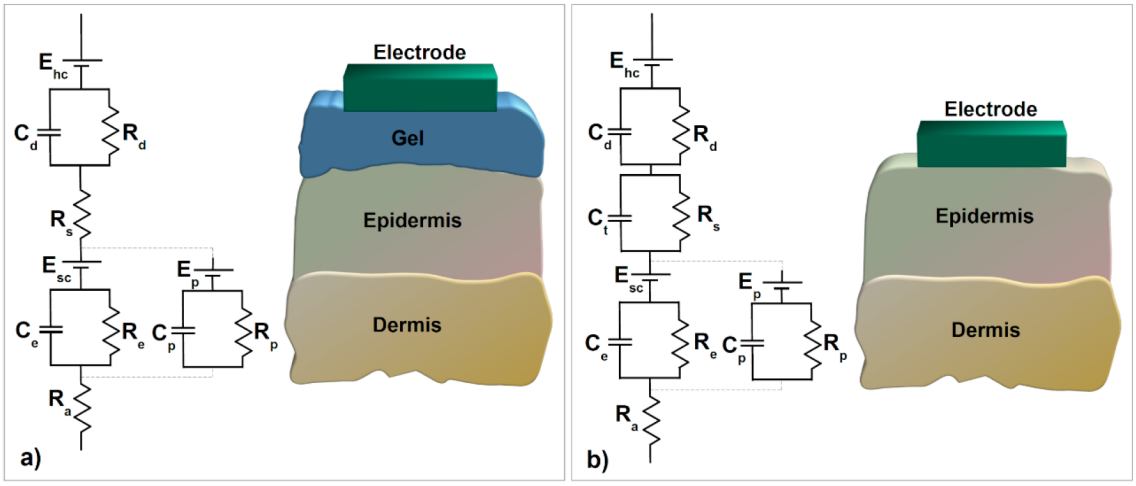

Figure 3.3 Equivalent circuit of skin–electrode interface for (a) traditional wet electrodes and (b) textile electrodes [44]

The equivalent circuit of the skin-electrode interface (Fig.3.3a) starts with electrode half-cell potential E_{hc} followed by the electrode-electrolyte interface between the electrode and the gel, which is represented by capacitance due to electrical double layer formation C_d and charge transfer resistance R_d. The gel medium is modeled by a series resistance Rs. The upper layer of epidermis behaves as a semipermeable membrane, which causes the difference in ion concentration and a potential difference, which is shown with E_{hc}. C_e andR_e models the impedance of epidermal layer and R_a models the dermis which behaves as a pure resistance.

Moreover, E_p, C_p, and R_p stand for the effect of sweat glands as a parallel conduction path through epidermis [50]. The half-cell potential appears as a DC baseline on the biopotential signals, is a particularly important contributing factor to the design decisions of any physiological signal acquisition unit development. This is due to its fluctuation, which varies even with a relatively little movement between the electrode and skin, which is interpreted as a noise like an artifact. Textile electrodes were believed to show a strong capacitive behavior compared to the conventional electrodes owing to the absence of electrolyte. Fig.3.3b illustrates this effect with capacitance C_t parallel to R_s, which herein C_t is in inverse proportion with sweat and the moisture over the skin [51]. Additionally, ambient humidity or applied pressure can be used to change moisture intensity [52]. Parallel RC blocks on the equivalent circuit imply that skin-electrode impedance decreases with increased frequency. The relation between the acquired output signal and in body biosignal means that lower frequency components of the biosignal will deviate more than the original. Decreasing the skin-electrode impedance, therefore, improves the signal quality.

One way to decrease the skin-electrode impedance is by moisturizing the inter-

face either with a hydrogel or salty water. Since a membrane interface improves the comfortability of the electrode, instead of salty water, the hydrogel membrane seems preferable. The only drawback of such a technique, however, is the bactericide/fungicide effect, which causes skin irritation, but this issue could be avoided [53] optimizing the hydrogel membrane's pH value between 3.5 and 9 . The other ingredient which affects the skin-electrode interface is the electrode's overall size, which presents an inverse relation with skin-electrode impedance [54]. Also, studies suggested that the applied pressure to the skin leads to lower skin-electrode impedance by providing better skin-electrode coupling [55].

Motion artifacts, identified as an undesirable signal in biopotential monitoring systems, occurs by any motion due to movement of one part of a section with respect to another (e.g., movement of connecting cables, patients' head) and can be categorized in few main sources [56]: (1)Measurement of an unrelated biopotential signal; for instance, electromyography (EMG) interferences in electrocardiography (ECG) recording. Proper electrode placement usually can avoid such interference. (2) Stretching of the skin leads to variations in the skin potential. In the textile electrode-based system, the fixation of the electrodes relies on the applied pressure, which is in a direct translation to the skin stretch. For reducing such motion artifacts, the applied force could be distributed to a bigger area than the electrode by the usage of a supporting structure surrounding the electrode [57]. (3) Cable bending generates friction and deformation on the cable isolator that results in triboelectric noise. A textile substrate could be enabled to reduce this effect to secure cables and the acquisition system into a garment, which could stream its information wirelessly.

3 EMG Applications with Smart Garments

EMG could benefit from textile platforms' advantages since they enable data acquisition in more realistic, casual, and out-of-lab settings. Research on EMG recording with textile electrodes either focuses on showing the feasibility of new electrode designs for the desired application or studies the proof-of-concept of an embedded textile electrode in wearable smart garments. Some of the popular application areas enabled by the acquisition of EMG with textile electrodes include muscle status monitoring [58, 59, 60], prosthetics [61, 62], and rehabilitation [63]. Other possible uses of wearable EMG platforms with integrated textile electrodes have also

been demonstrated, including running leggings for muscle fatigue detection (Figure 3.4a-c) [16]; shorts for energy expenditure analysis [64] and ventilatory threshold estimation [10]; eye glasses for the analysis of chewing cycle [65]; and a shirt for athlete training (Figure 3.4d-f) [58].

Figure 3.4 Wearable electromyography (EMG) acquisition garments: running leggings and a sports shirt. Electrode placement in the (a) exterior; and (b) interior of leggings; (c) actual view of leggings when worn by a subject [16] ;(d) shirt as worn by a subject; (e) location of electrodes on the shirt; (f) close-up view of the acquisition unit attached to the shirt [58].

The concept of a compression garment with integrated EMG textile electrodes was recently commercialized by two companies: Athos (Mad Apparel Inc., CA, US) and Myontec (Myontec Ltd.,Kuopio, Finland). Both are mainly focused on athlete training, with Myontec also advertising their products for the rehabilitation and ergonomic studies. These types of EMG wearables could also find an appeal among amateur sports enthusiasts for prevention of personal injuries since it was documented in 2014 that $33Bs were spent on sports injuries of young adults and 50% of this injuries were preventable [3]. It is anticipated that, with the advances in wearable computing, similar products will emerge at a competitive price in the near future and possibly offering additional capabilities.

IV. GRAPHENE TEXTILE WEARABLES FOR EMG

One of the obstacles on the way of broader use of textile electrodes is their fabrication cost. Approaches such as electroplating, screen printing, or knitting for the fabrication of conductive textiles have limited scalability due to their equipment or process demands. As a solution to this problem, our team developed conductive graphene textiles with a dip-coating method, which is scalable and adaptable to commercial textile fabrication processes. Then, the utilization of graphene textiles as electrodes was also done, and it was studied for cardiac and ocular potential acquisition with creating respective wearables [18, 66]. As a continuation of previous works, in this section, the creation of a wearable platform for EMG acquisition will be explained with starting from conductive graphene textile fabrication up to graphical user interface level.

1 Preparation of Conductive Graphene Textiles

Graphene-coated conductive textiles were prepared by following an inexpensive and scalable three-step dip-dry-reduce process [42] so that conformal cladding of graphene over textile fibers could be obtained. The process started with the synthesis of graphene oxide (GO) solution with the modified Hummer's method. Then, the desired piece of nylon was dipped into GO solution and left to dry on a hydrophobic Teflon surface afterward (Fig.4.1a-b). At this point, GO flakes were stable on nylon fibers, and the subsequent reduction of GO with a reducing agent (e.g. hydrazine or hydrogen iodide) provided conformal coating of graphene on nylon (Fig.4.1c). Following reduction, textiles were intensively rinsed with water to wash away any chemical residue. Although reduction could be performed thermally, the possibility of disintegration of textiles in high temperatures and low adsorption of graphene to cellulosic fibers makes coating with GO solution and its chemical reduction more

appealing [67]. End conductivity achieved with chemical reduction is dependent on various factors such as type of the reduction agent, its concentration, duration of the reduction reaction, type of the textile. The three-step dip/dry/reduce approach described herein was successfully applied to a variety of ordinary textiles with the hydrophilic surface property, including polyester, nylon, cotton, Kevlar. Among these, nylon was chosen for its small surface roughness, which allows a better connection between graphene flakes on fiber surfaces and a better conductive network on the textile surface.

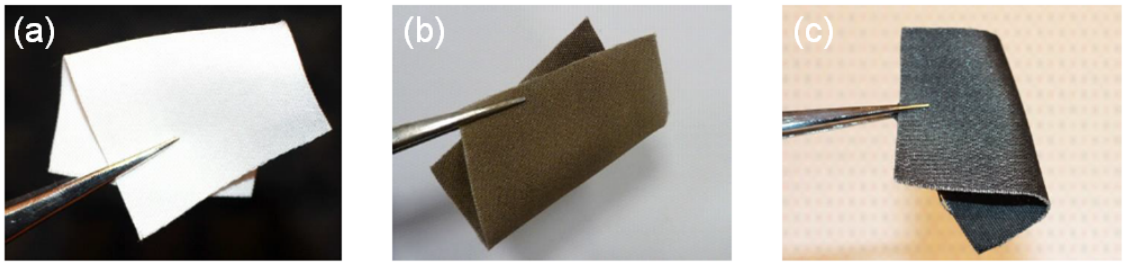

Figure 4.1 Textile fabrication process. (a) Plain textile (b) GO coated textile (c) Textile after the reduction [18]

After the reduction, the conductivity of the textiles was assessed with a four-point probe measurement where sheet resistivity and conductivity were found as 13.96 k Ω/square and 0.325 S/m, respectively with a thickness of 0.2 mm.

2 Creation of Textile Electrodes

2.1 Development of the Electrodes

The prepared conductive textiles were cut into smaller pieces of 1.5 x 1.5 cm and attached to flexible foam backings to obtain approximately the same area with conventional $3M^{TM}$ foam monitoring Ag/AgCl electrodes used in this study (i.e. diameter of 1.7 cm and active sensing area of 2.3 cm^2). This rendered to have a size above SENIAM recommendation along with the muscle fiber, and it was decided to be acceptable after trials showed no significant cross talk coming from neighboring muscles. Snap fasteners were used to provide electrical interfacing (Fig. 4.2).

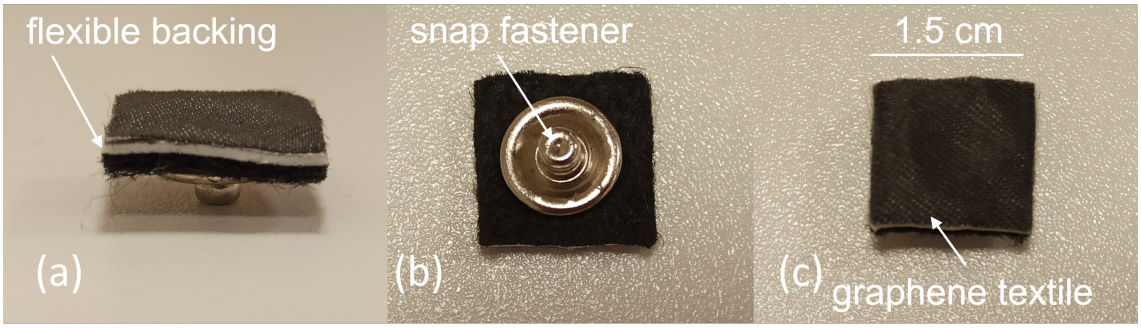

Figure 4.2 Fabricated textile electrode from different perspectives.

2.2 Characterization of the Electrodes

Skin-electrode impedance may be considered as a critical quantitative indicator of electrode performance [44], where lower and more stable impedance values imply better signal quality. It was, therefore, meaningful to start the comparison of Ag/AgCl and graphene electrodes by comparing their respective skin-electrode impedance values. A separate measurement setup was constructed, referring to the previous literature [68]. Three electrodes were placed on the forearm with 5 cm distance between them Fig.4.3 and a Howland current pump was constructed to supply an AC current that has a constant amplitude of 10 μA and variable frequency in the range of 1Hz-500 Hz. Impedance values up to 500Hz were recorded since it's the relevant frequency band for sEMG power spectrum.

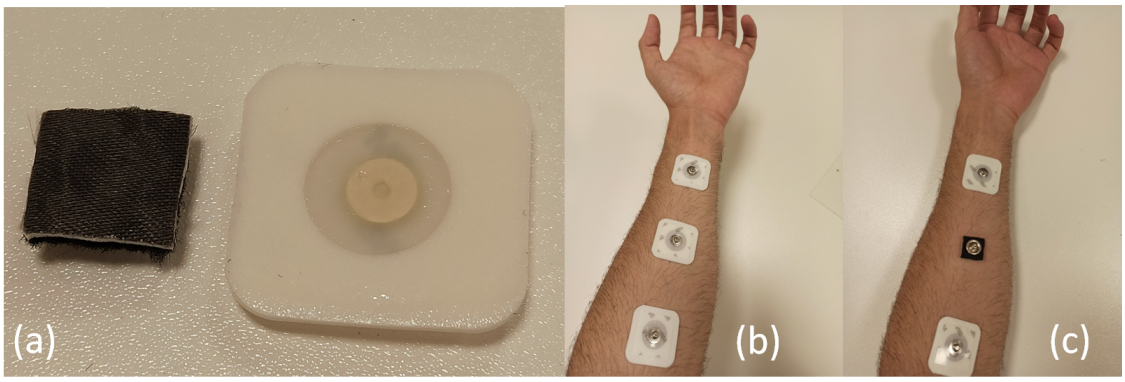

Figure 4.3 3 (a) Textile and clinical electrodes with similar active region areas; Electrode placement for (b) Ag/AgCl ; (c) Gr electrode skin-electrode impedance recordings

As seen from Fig.4.4, impedance values of the prepared textile electrodes are bigger than the Ag/AgCl electrodes; however, their results were accepted to be inside of a

reasonable range for textile electrodes which can go up to several hundred-kilo ohms. There are also two interesting regions on the graph to compare the impedance values. The first one is at the power line frequency of 50 Hz where 31,6 kΩ and 49,4 kΩ impedance values were found respectively for clinical and textile electrodes. This indicated more susceptibility to power line noise for textile electrodes, which can jeopardize the available information with saturating the amplifiers or lowering the SNR value. It can be compensated with a careful choice of analog front end and digital filtering. The second region is the lower frequency portion of sub 5 Hz where motion artifacts are present. From 1 Hz to 5 Hz Ag/AgCl impedance was about 50 kΩ on the other hand textile was about 90 kΩ. For the recordings done with textile electrodes compared against clinical electrodes, it's evident that contamination from low-frequency motion artifacts will be relatively more than power line interference. Because of that, this frequency portion should be eliminated early in the analog conditioning phase, and motion artifacts should be restricted with stable electrode-skin contact.

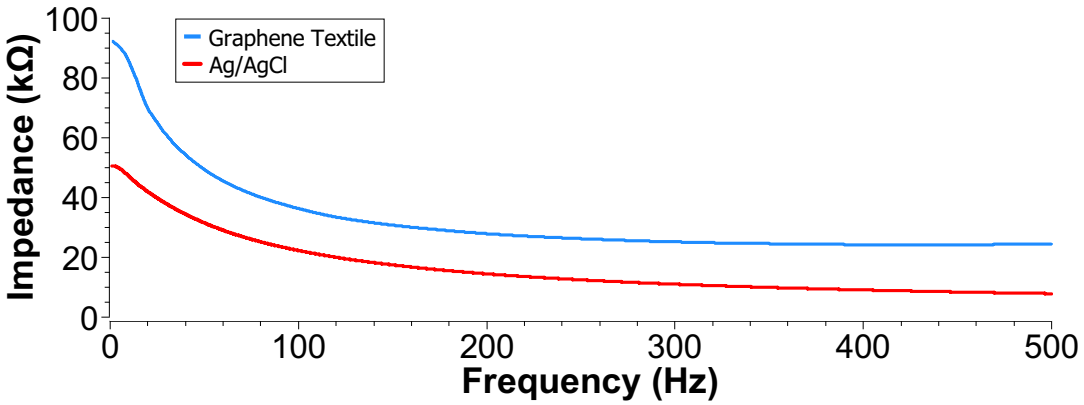

Figure 4.4 Skin-electrode impedance comparison between Gr and Ag/AgCl electrodes.

3 Performance Comparison with Static Trials

After gaining insides on the electrode performance with skin-electrode impedance comparisons, evaluation of signal qualities for clinical electrodes and textile electrodes in constrained movement scenarios were conducted. Although the final target of this project is to come up with a battery-powered wireless acquisition unit, for the electrode performance comparison in the static acquisition scenarios, an acquisition

unit powered from a power supply that also sends data by a USB cable was used.

The static acquisition unit starts with the analog conditioning part, which needs to condition the noisy signals picked up by the electrodes. An unamplified sEMG signal from surface electrodes typically has an amplitude between a few μV to 3 mV, and its frequency spectrum ranges between 6–500 Hz while a bigger portion of the energy lies in the interval of 20–150 Hz [69]. Biggest noise sources also have a known spectrum at 50 Hz with power line interference and sub-10 Hz with motion artifacts [70]. Analog and digital filtering, together with a reasonable amount of amplification, needs to be provided to get the most information out of the acquisition.

Referring to the Fig.2.3, signals picked up by the electrodes were conditioned through an analog front-end before being fed to the analog to digital converter. The designed circuitry mainly consisted of an instrumentation amplifier (INA128, Texas Instruments) followed by a 2nd order high-pass and 4th order low-pass filters with Sallen-Key Butterworth topology to achieve 10–500Hz passband without any other hardware filtering. Total amplification of 1120 V/V was reached with combining input gain of INA128 with an additional gain block after the filters (Fig.4.5). It has the same design with a previous work done by our group on electrooculagraphy acquisiton [71], where analog filter band is now adjusted for

Visual inspection during data acquisition and digital processing of the signal afterward was performed in MATLAB Simulink environment (Mathworks, Natick, MA, USA). An Arduino Uno board interfaced with the Simulink was used for ADC, digital conditioning, and visualization. The sampling frequency was set to 1100 Hz ensuring accurate signal acquisition without significant aliasing. Signal processing of the acquired raw data starts with the application of a comb filter to kill 50 Hz noise and its harmonics. Then, it is followed by digital attenuation of the signal to cancel the circuit gain, which estimates the sEMG signal level picked up by the textile electrodes.

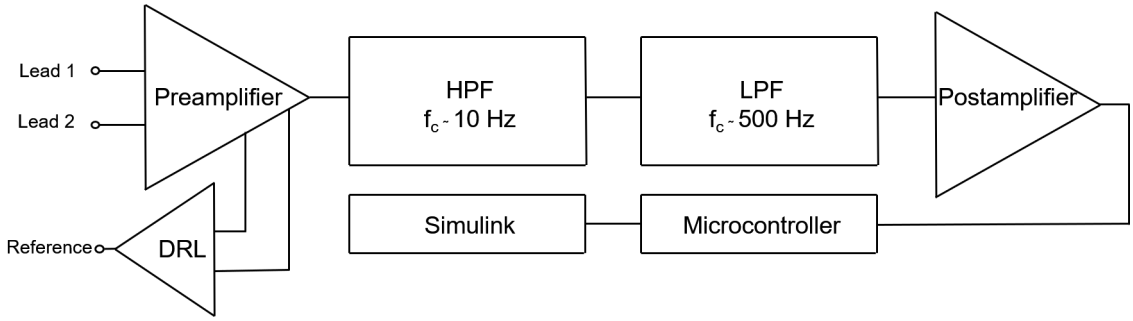

Figure 4.5 Block diagram of the first acquisition unit.

All the trials were done with the participation of a 25 years old healthy male subject.

Bipolar electrode couple was placed through elastic bands with 2 cm inter-electrode distance on the right arm for biceps brachii, triceps brachii muscles, and on the right thigh for quadriceps femoris muscle. The selection of the elastic bands was also important to provide enough pressure to ensure good coupling between skin and electrode [72].

Experiment protocol consisted of a 5 seconds contraction, followed by 5 seconds relaxation cycle repeated five times. Dumbbells of 1, 2, and 4 kg, which were bought prior to the experiments, were used for contracting the biceps brachii and triceps brachii muscles. The contraction of quadriceps femoris is achieved with squat exercise (Fig.4.6). Trials were started 10 minutes after the application of the electrodes to avoid a change in the signal quality due to sweat.

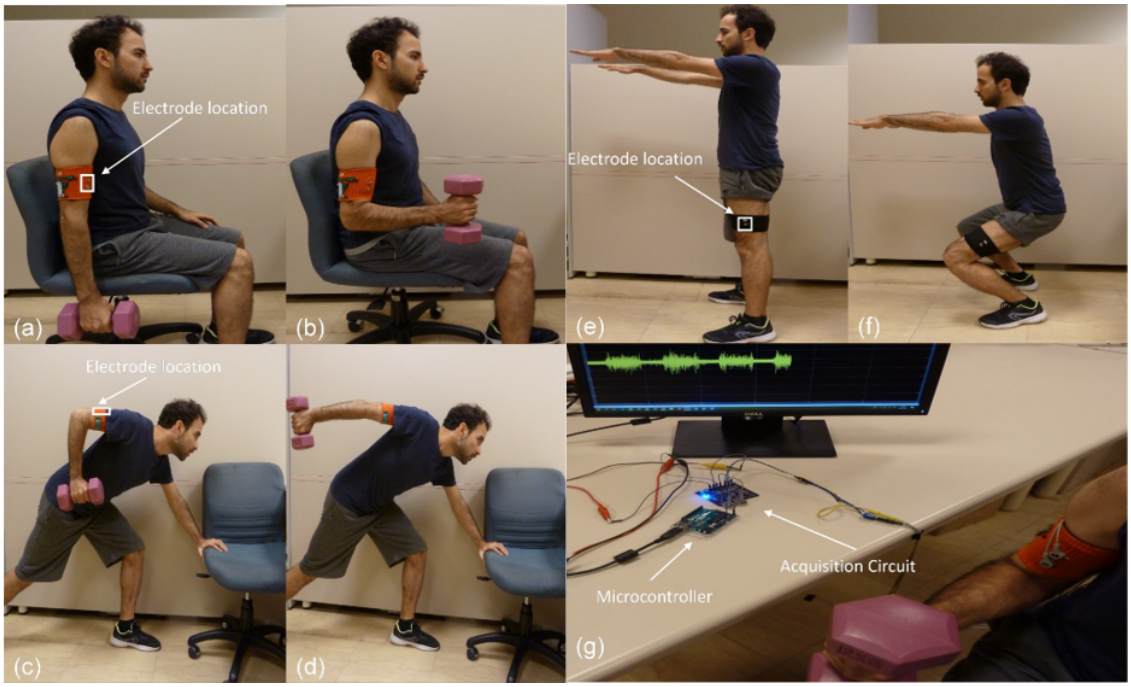

Figure 4.6 Images of performed exercises with specified electrode locations (a), (b) relaxation and contraction of biceps brachii; (c), (d) triceps brachii; (e), (f) quadriceps femoris. (g) An instance from data acquisition.

Due to the physiology of muscle contractions, sEMG bursts cannot be precisely reproduced in its previous shape; therefore, the recorded sEMG signals displayed random fluctuations preventing direct comparison of the acquired signals (Fig.4.7a). Implementation of digital smoothing to grasp the mean trend of the signal is a viable solution to this problem. Root mean square (RMS) filter is a recommended smoothing algorithm since it reflects the mean power of the signal [69]; accordingly, a 200 ms window was applied for smoothing (Fig.4.7b).

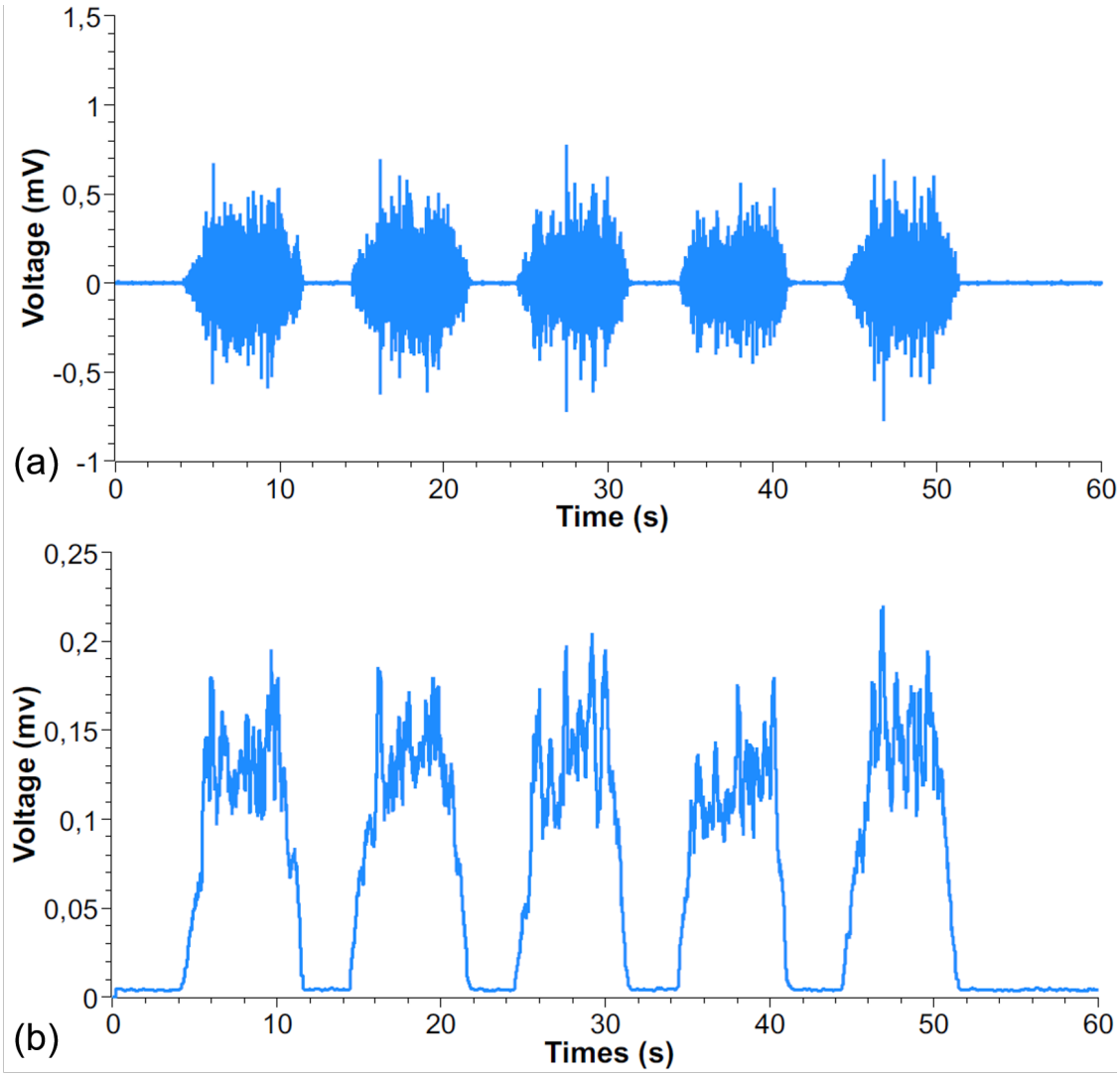

Figure 4.7 sEMG signal taken from Quadriceps (a) original signal, (b) signal after moving RMS smoothing.

After smoothing, cross-correlations between the signals recorded from Ag/AgCl and graphene electrodes were calculated (Table IV.1). A high correlation coefficient of 0.95 on average was observed for all trials. Fig. 4.8 shows the similarity and excellent overlap between the envelopes of the sEMG bursts with 2 kg weight after the application of RMS. As an important quality measure, SNRs were also determined by implementing the algorithm described by Agostini et al. for cyclic sEMG signals that enable the automatic calculation of SNR [73]. Table IV.1 shows that SNR values revealed similar signal qualities for both electrode types.

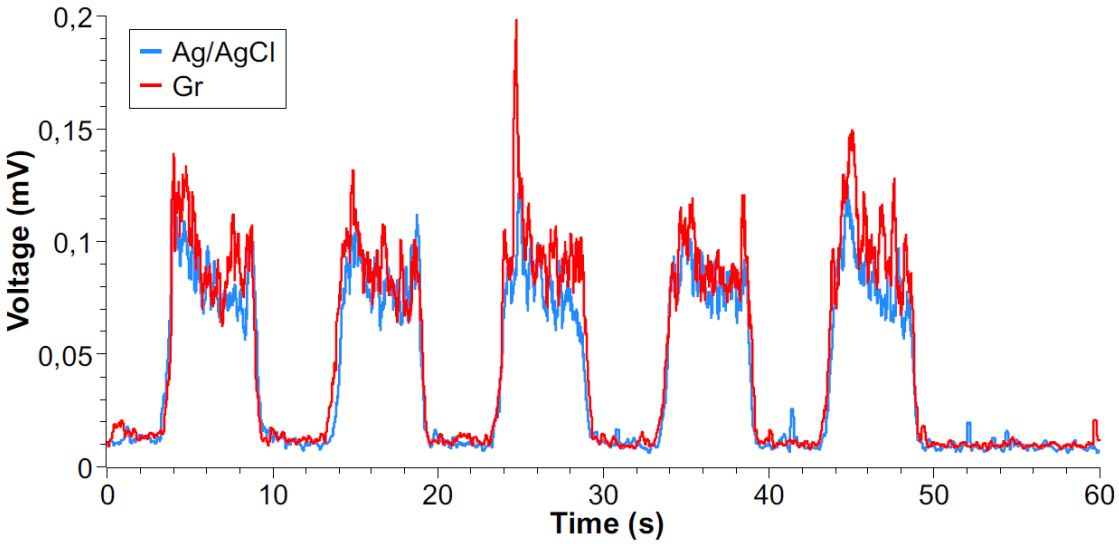

Figure 4.8 Comparison of triceps brachii signals for 1kg weight exercise, cross correlation above 0.98 is observed.

Table IV.1 SNR And Cross Correlation Values

Muscle	Weights	Ag/AgCl SNR	Graphene SNR	Cross Correlation
Triceps	No Load	15.58	14.70	0.9782
	1 Kg	18.52	17.77	0.9849
	2 Kg	19.58	19.23	0.9792
Biceps	No Load	21.16	21.32	0.9505
	1 Kg	22.83	23.87	0.9412
	2 Kg	27.66	27.18	0.9680
Quadriceps	Squat	32.85	28.13	0.9694

In addition to these experiments where the same exercises were conducted in different periods of time with a single channel acquisition unit, a side by side comparison with a multichannel commercial data acquisition unit (OpenBCI, Cyton board) was performed. Two channels were placed symmetrically across biceps brachii. At first, two of them were chosen with Ag/AgCl electrodes to match the acquired signal quality (Fig.4.9a), then one of the channels was replaced with graphene electrodes (Fig.4.9b). For assessing the SNR values, the previous cyclic exercise method was followed with a 2 kg dumbbell.

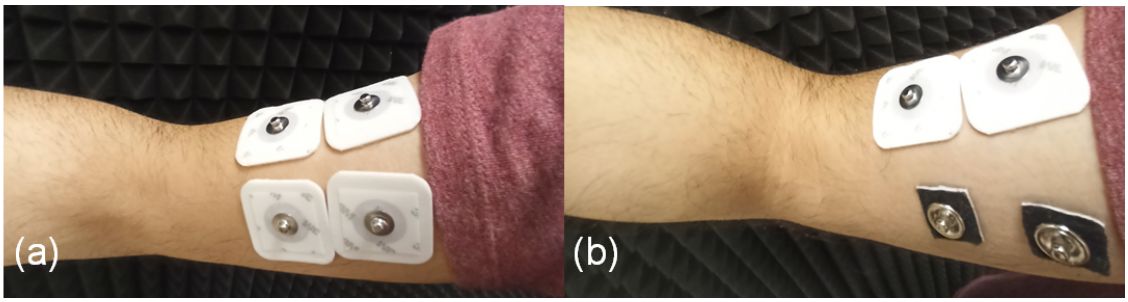

Figure 4.9 Electrode placements on the biceps brachii for side by side comparison.

Comparisons performed in two different times revealed average SNR values of 15,06 for Ag/AgCl and 9,58 for graphene electrodes. These revealed a performance value around 65% for textile electrodes as opposed to the similar values seen with previous static experiments. This swing in the performance can be attributed to the difference in the applied pressure level (affects the conformality of the contact) or difference between the textile electrodes (variation in textile conductivity) used in static experiments and side by side trials. Due to the small sample space of the conducted comparisons, it is not practical to deduce a decisive result about the repeatability and variation of the performance levels. Nevertheless, even the worst-case performance of the textile electrodes seems to be reasonably well for integration into wearable garments.

4 Mobile Acquisition Unit

As the capstone of this study, sEMG information was desired to be used in the wearable application level. This is required to upgrade the prototype in the previous section to a battery-powered wireless solution. Structure of the analog circuit stayed the same except the filter bandwidth is moved to 60-300 Hz, which was found to carry enough information for the desired application, while providing an analog filtration to 50 Hz mains hum.

Changing the instrumentation amplifier and opamps to single supply equivalents INA122 and OPA365 enabled the use of battery. As the battery a 500mAh Li-Ion battery of 3.7V was used, which was managed with MCP73831(Microchip, USA) charge management controller. Microcontroller used for ADC conversion was changed from Arduino Uno to Arduino Pro Mini, and rail splitter TLE2426 (Texas Instruments, USA) was used to add the half rail to the analog signal to make it

readable in its entirety by the ADC of the microcontroller.

In the end, sEMG signals starting from textile electrodes up to storage and data display travels the following path. Signals picked up by the bipolar electrode pair first enter a precision instrumentation amplifier (INA122, Texas Instruments) with a high common-mode rejection ratio (CMRR), which was necessary for separation of low amplitude biopotentials from huge common-mode noise. INA122 has CMRR of 96 dB, and the fact that it can operate with a single supply was important for battery-driven applications. An adequate pre-amplification was also applied in this stage by tuning the gain resistor for the desired level. Also, there is a driven right leg (DRL) circuitry branch to provide a negative feedback loop for the common-mode voltage and minimize it as much as possible [74]. After the instrumentation amplifier, analog signal needs to be conditioned for ADC conversion and subsequent digital processing. In the acquisition circuitry, the 10 bit ADC of preferred microcontroller was employed. This means that ADC doesn't have the capability to differentiate features smaller than 5 μV, and the signal requires amplification to preserve valuable information. Motion artifacts, however, present themselves mostly as baseline noise that has a bigger amplitude than the target signal. Direct post-amplification of the signal after the instrumentation amplifier causes saturation. Therefore, filtering of this low-frequency motion artifacts with high pass filtering is required. Then, a programmable gain amplifier (PGA) stage was constructed with MAX5421 programmable voltage divider. This allows us to change the gain of the circuit between some predetermined values with software control. Prior to ADC, analog low-pass filtering is required for anti-aliasing. In the end, a 2nd order high-pass filter and 4th order low-pass filters with Sallen-Key Butterworth topology were chosen to achieve the 60-300Hz passband. An amplification value between around 500-2000 V/V was reached with combining input gain of INA122 with the programmable gain after the filters (Fig. 4.10). The acquisition unit design used herein is the same as the one done for mobile EOG acquisition by our group [75].

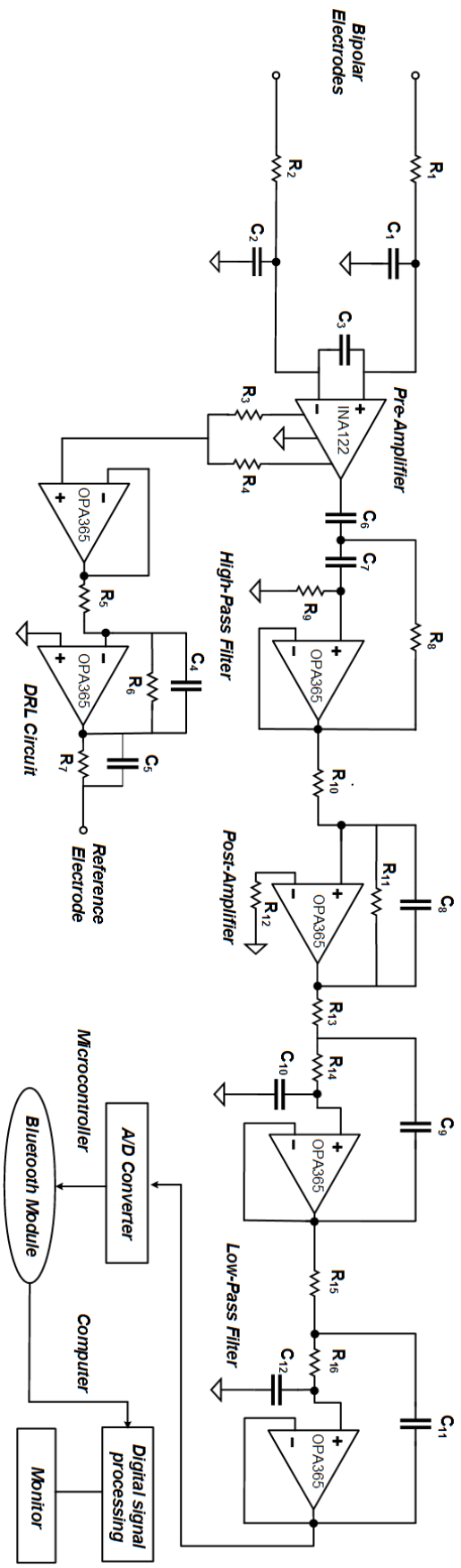

Figure 4.10 Signal acquisition unit from electrodes to monitor where analog conditioning part was shown explicitly.

After the analog conditioning part, the signal arrives at the Arduino Pro Mini board, where it is converted to the digital domain in ADC of ATmega328 microcontroller. The sampling rate was set to 1000 Hz, which avoids aliasing from EMG signal that was band-limited to 300 Hz with the low pass filter. Then, the signal was sent wirelessly to a laptop through an HC06 module, which allows inexpensive short distance Bluetooth communication. This was the key to freeing the acquisition unit from cable communication with computers and achieving a mobile wireless system. In the end, there were to separate printed circuit boards (PCB): one carrying the analog front end and the other carrying the microcontroller, the Bluetooth module, and the power module (Fig.4.11a). They were mounted on top of each other through headers to end up with a smaller footprint for the whole system. (Fig.4.11b) Also, a custom case for the acquisition unit was fabricated with laser cutting plexiglass sides and then gluing them accordingly (Fig.4.11c).

In the computer, digital processing and visualization were done in the LabVIEW graphical programming environment. Digital signal conditioning starts with cleaning of 50 Hz noise and its harmonics through a comb filter. It is followed by a digital attenuation to cancel the analog gain, which estimates sEMG signal amplitude picked up by textile electrodes. Also, a graphical user interface was prepared in LabVIEW to improve the data representation and user experience (Fig.4.12). In the end, the whole acquisition unit costs around 100 dollars, which is five times more economical than the cheapest commercial alternative in the market.

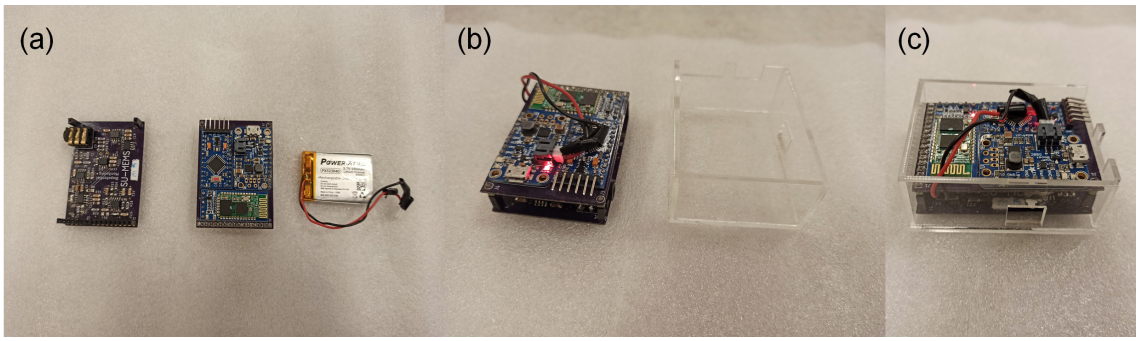

Figure 4.11 Mobile acquisition unit (a) top/down PCBs and Li-Ion battery (b) assembled acquisition unit with transparent case (c) acquisition unit placed inside the case.

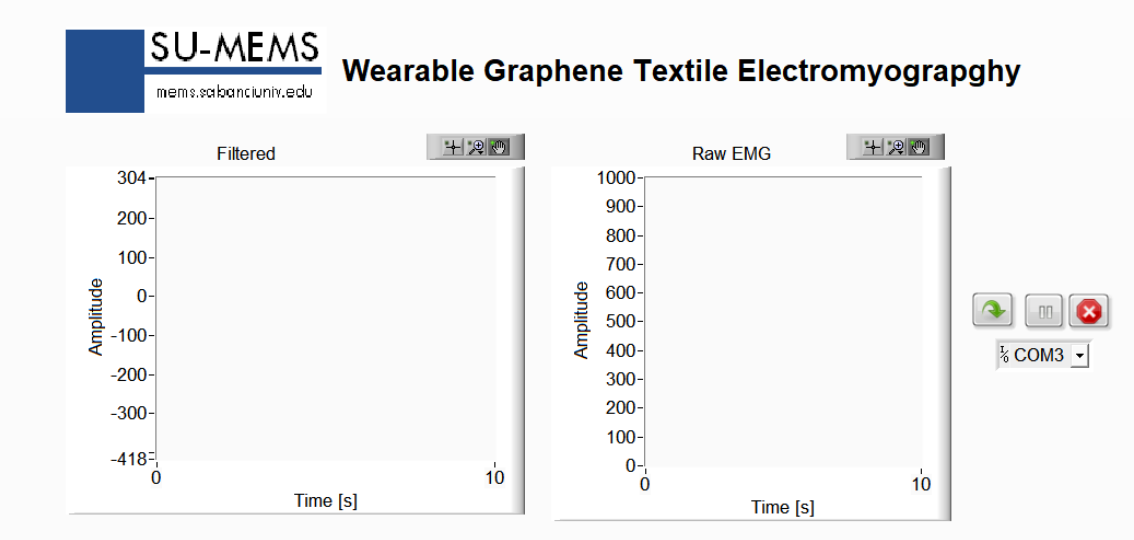

Figure 4.12 Graphical user interface created in the LabVIEW.

V. TESTING OF THE WEARABLE GRAPHENE TEXTILE sEMG MONITORING SYSTEM IN DYNAMIC CONDITIONS

1 Step Counter

In the times of self-isolation and social distancing that the world is going through with the Covid-19 pandemic, a significant chunk of the population is experiencing less daily physical activity than their pre-pandemic level. Although the health benefits of physical activity are well known by society, regular exercising is not an easy task. It is known that using the wearable activity trackers for assisting or for intervention could positively increase the daily physical activity of the user [76].

Pedometers are one of the most popular activity tracking methods also used in on our cell phones and they are based on the build-in MEMS accelerometers the use of pedometers (step counters). Creating a pedometer functionality with a wearable garment paradigm is interesting since it directly allows us to follow the electrical activation of muscles involved in walking. One of the main skeletal muscles that is activated during walking or running cycles is peroneus longus muscle, which empowers various foot and ankle movements [77]. Creating a calf band with specific electrode placements for peroneus longus and a pocket to carry the acquisition unit enabled the wireless monitoring of the EMG signals. Subsequent processing of the acquired signals in LabVIEW was used to count the steps taken.

The design of the calf band was a trial and error process that included trying out different types of fabrics, electrode placement, and sewing. In the first iteration of this process, a single bipolar electrode couple was created on a piece of regular fabric that later cut down to the width of the elastic band, which was used to make the calf band skin tight and provide enough pressure to fixate the electrodes. Electrode carrying textile, elastic bands, and velcro bands were all sewn together to create the

calf band (Fig.5.1).

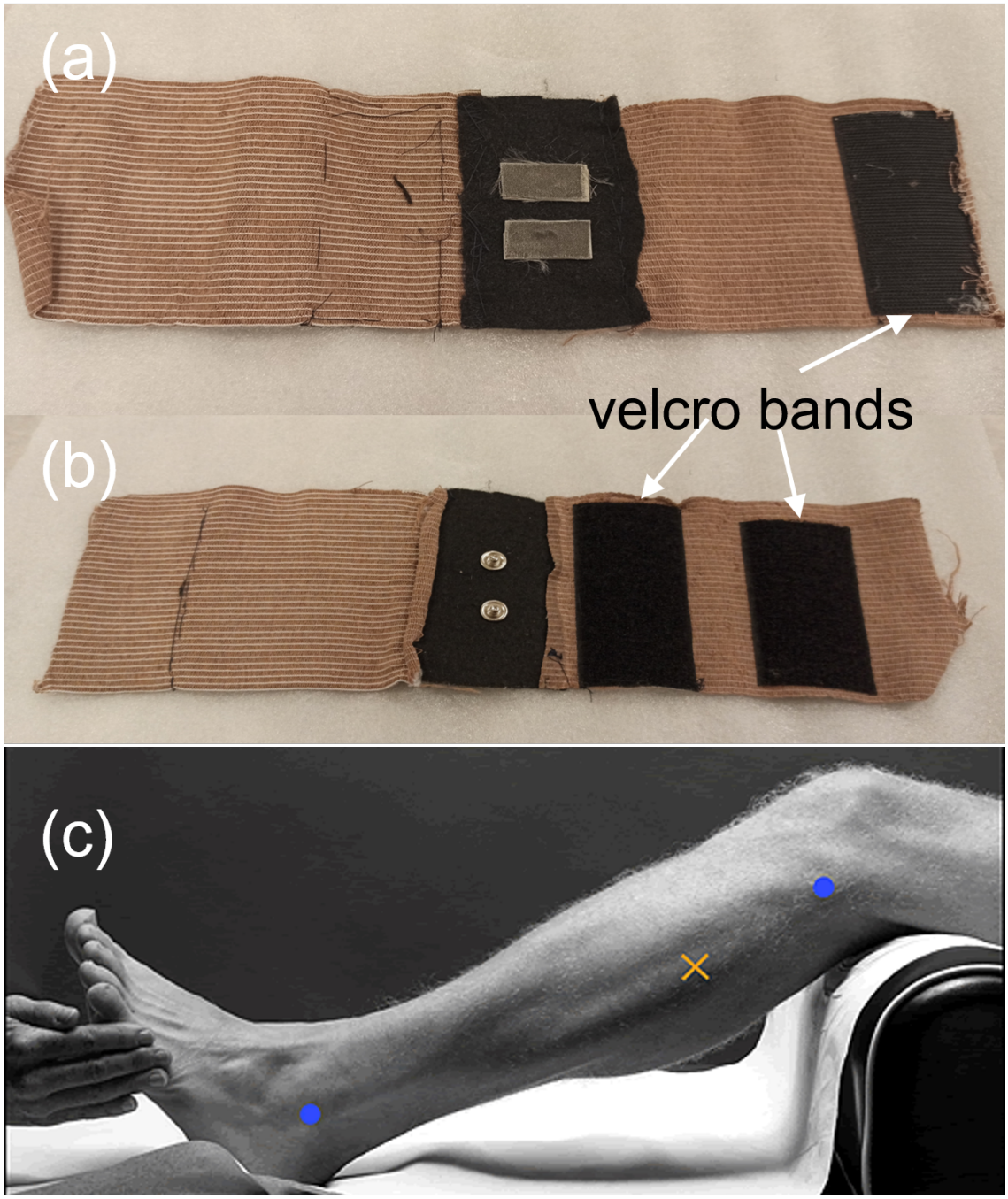

Figure 5.1 (a) Front side of the first calf band and (b) back side (c) Peroneus longus position, indicated with muscle belly and end points [78].

After placing a Ag/AgCl electrode as the reference, it was seen that the signal quality was promising for a pedometer application. In the second iteration, the calf band was modified to become completely wearable by creating a third textile electrode for reference and a pocket to carry the acquisition circuit. The electrode couple was positioned on top of the peroneus longus, and the reference electrode was placed

on the skin surface closest to the tibia. Additionally, elastic band color was also changed to black to match better with regular fabric color (Fig.5.2).

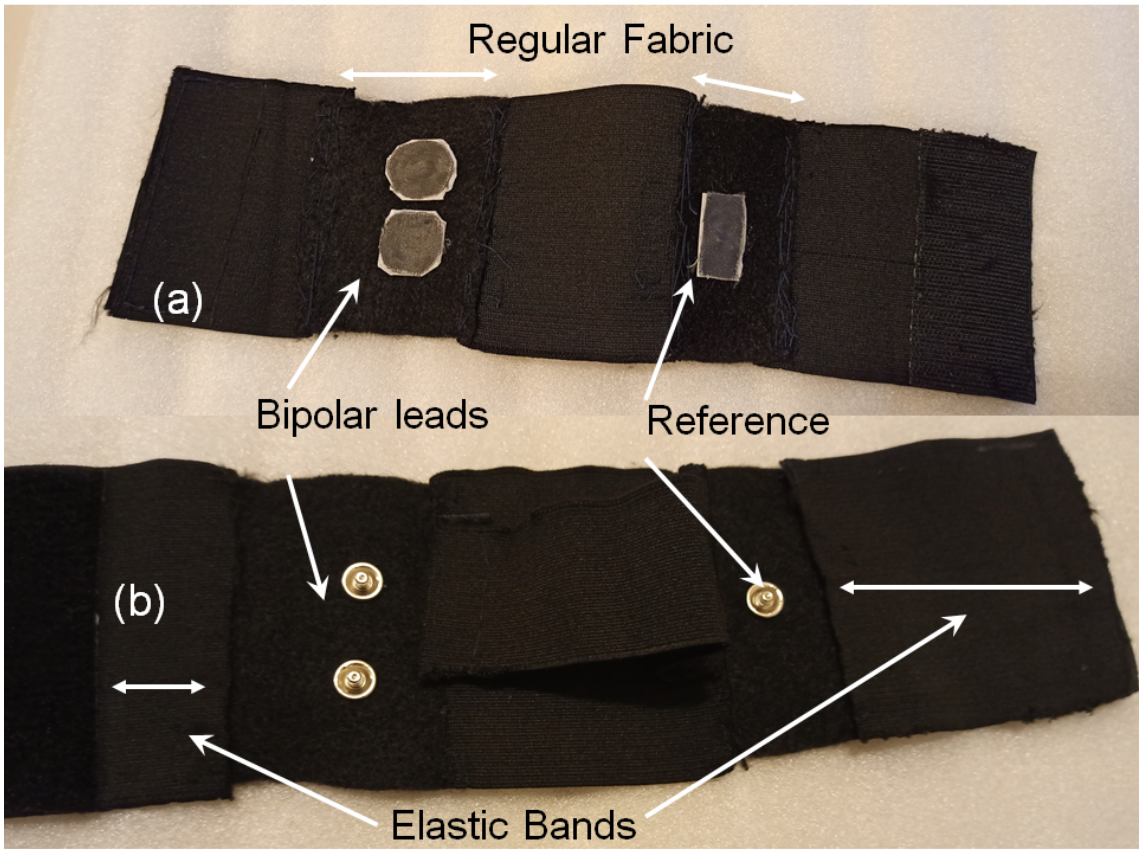

Figure 5.2 Second iteration of the textile embedded calf band. Bipolar electrode couple and reference electrodes are placed on different piece of fabrics. Connecting elastic bands and electrode carrying fabrics are sewn together to obtain a one piece band.

For the last iteration of the calf band, two improvements were thought. Placing all three electrodes on the same regular fabric to be able to exert more pressure from the elastic band and playing with the orientation of the bipolar electrode couple to have a better coupling. In this case, the bipolar electrode couple was tried to be placed on muscle belly whereas the reference electrode was placed near muscle tendon (Fig.5.3)

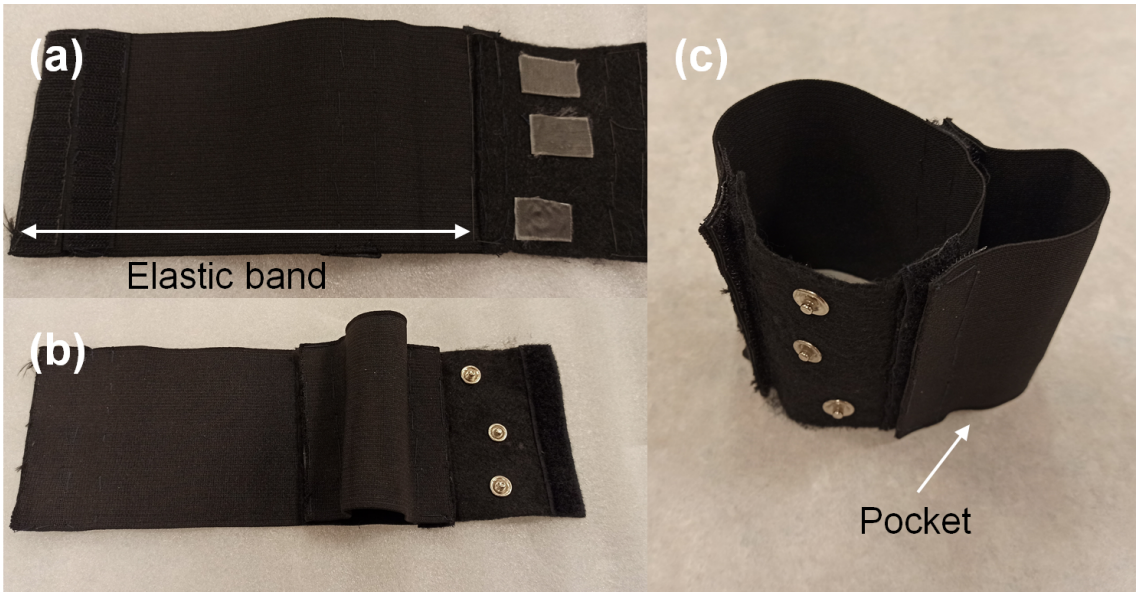

Figure 5.3 Third and final iteration of the calf band, reference lead was placed in the same regular fabric.

The step counting algorithm implemented here is about separating different instances of increased muscle activation from each other. Since only a single channel of just one muscle was used, for subtle movements like slow walking, it's hard to match individual steps with muscle activation. This is since single steps do not cause an abrupt change in slow-paced movements.

A treadmill was used to perform walking and running experiments for the developed step-counter. A test group of four people participated, who were requested to run for 5 minutes. During the experiment, they switched between three different fast walking/running speeds of 4, 6, and 8 miles for about 1.5 minutes (Fig. 5.4).

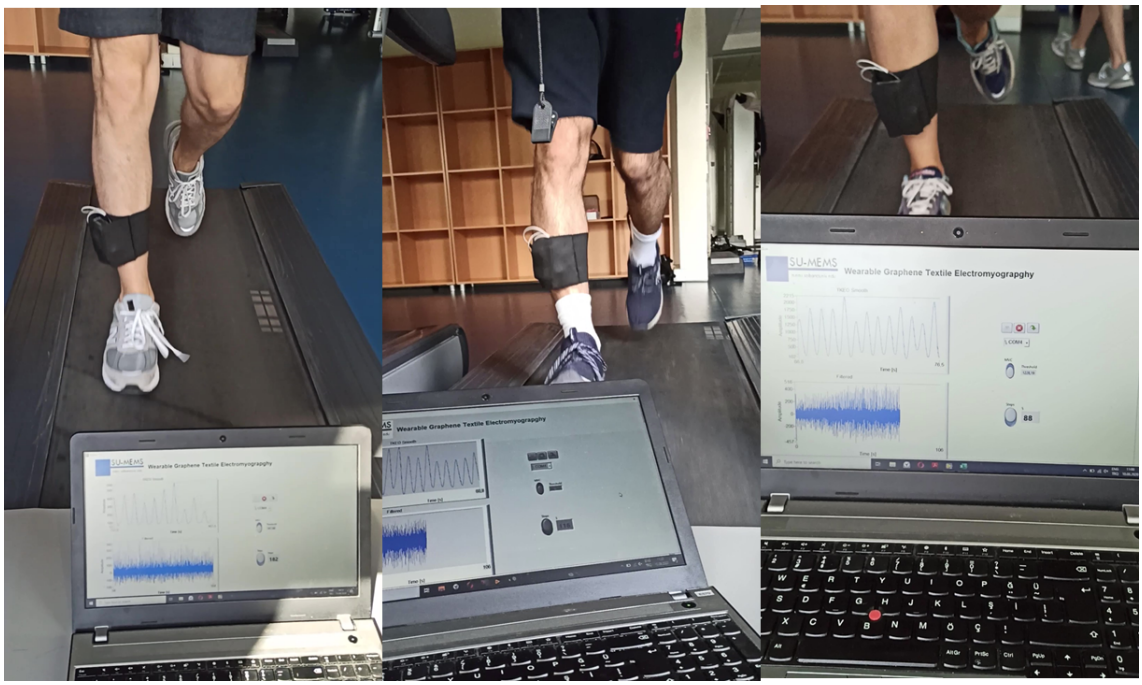

Figure 5.4 Three of the subjects together with user interface developed in the LabVIEW.

During the experiment, realtime data processing was performed simultaneously. The algorithm is about separating different instances of increased muscle activation from each other. After the standard removal of the power line noise and DC removal as well, Teager-Kaiser enery operator (TKEO) was applied to the signal. TKEO is a non-linear enery operator which was previously shown to improve the EMG burst detection performance [79]. It can be expressed as in (5.1).

$$\Psi[n] = x[n]^2 - x[n+1]x[n-1] \tag{V.1}$$

TKEO was first introduced by Kaiser to detect instantaneous amplitude changes in a time-varying monochromatic signals [80]. Later on, it was also utilized on broadband bio-signals to detect abrupt changes such as spike detection [81]. Since it reflects the energy changes coming from both instantaneous amplitude and instantaneous frequency, it is a useful tool for the detection of increased EMG activity, too [82]. Low computational complexity in return for improved signal to noise ratio presented by TKEO makes it an appealing choice for real time signal processing.

Acquired signal energy, then, was smoothed out three times with a median filter of 200 ms window. An automated threshold was applied to the signal to determine the muscle activation of peroneus longus muscle. The threshold was created and

updated by storing the last three seconds of the smoothed signal and using the average of maximum and minimum values of that array, as shown in (5.2).

$$Threshold = \frac{MAX_{3sec} + MIN_{3sec}}{2} \tag{V.2}$$

Since the number of steps taken by a single leg was calculated, it was multiplied by two to have an estimate of the total number of steps from both right and left legs (Fig. 5.5).

Fig. 5.5 shows an ideal working scenario where everything goes smoothly. SNR of the signal is big enough for detection, and motion artifacts are limited. However, during the experiment, unexpected variations occurred as well, is attributed to potential movement of the calf band (Fig.5.6a-b).

Such distortions may disrupt the step counting algorithm, and as it can be seen from Fig.5.6c-d, threshold detection in this abrupt change followed by low-quality signal caused a problem in counting. As the signal's baseline noise increased, three steps were miss counted; also low SNR part had extra step counting.

Correcting these mistakes to a certain degree is possible considering the cyclic nature of walking/ running; consecutive steps always will have a similar time interval between them (Fig.5.7a-b). Detecting and updating this interval length could enable understanding the extra and missed steps for the chosen signal where the subject was jogging in a constant speed of 6 mil/h; this interval was around one second. Dividing the detected intervals with this approximate step length and then rounding the number to the closest integer gives a better estimate of the total steps taken (Fig.5.7). When the real count was 22 without the correction algorithm, it counted as 19, and with correction the total step count was 21, indicated that only one step missed.

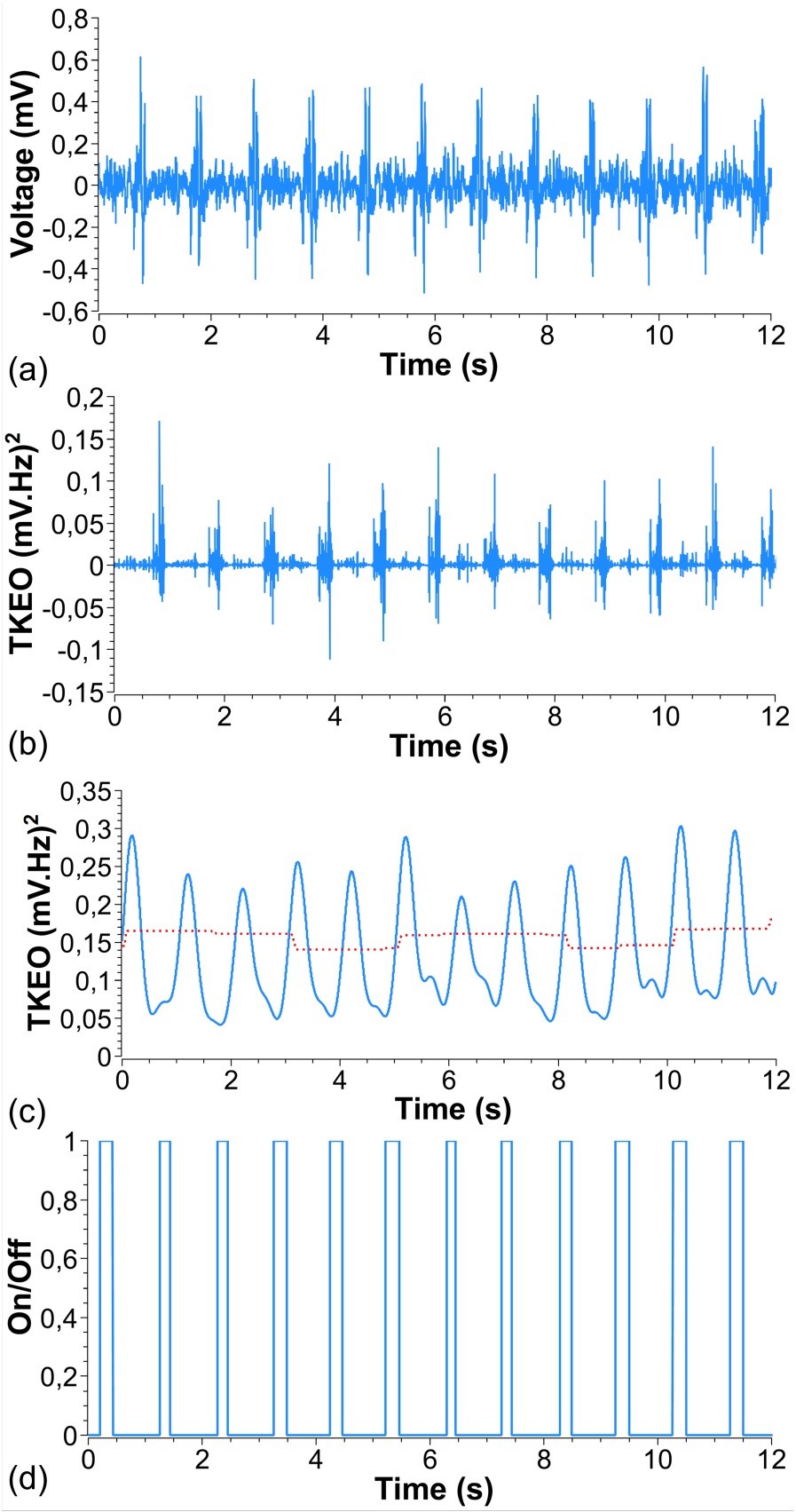

Figure 5.5 Step Detection algorithm (a) Raw signal (b) Signal after application of TKEO (c) Smoothing the signal three times with a median filter, red dash shows the adaptive threshold (d) Muscle activation instances passing the threshold.

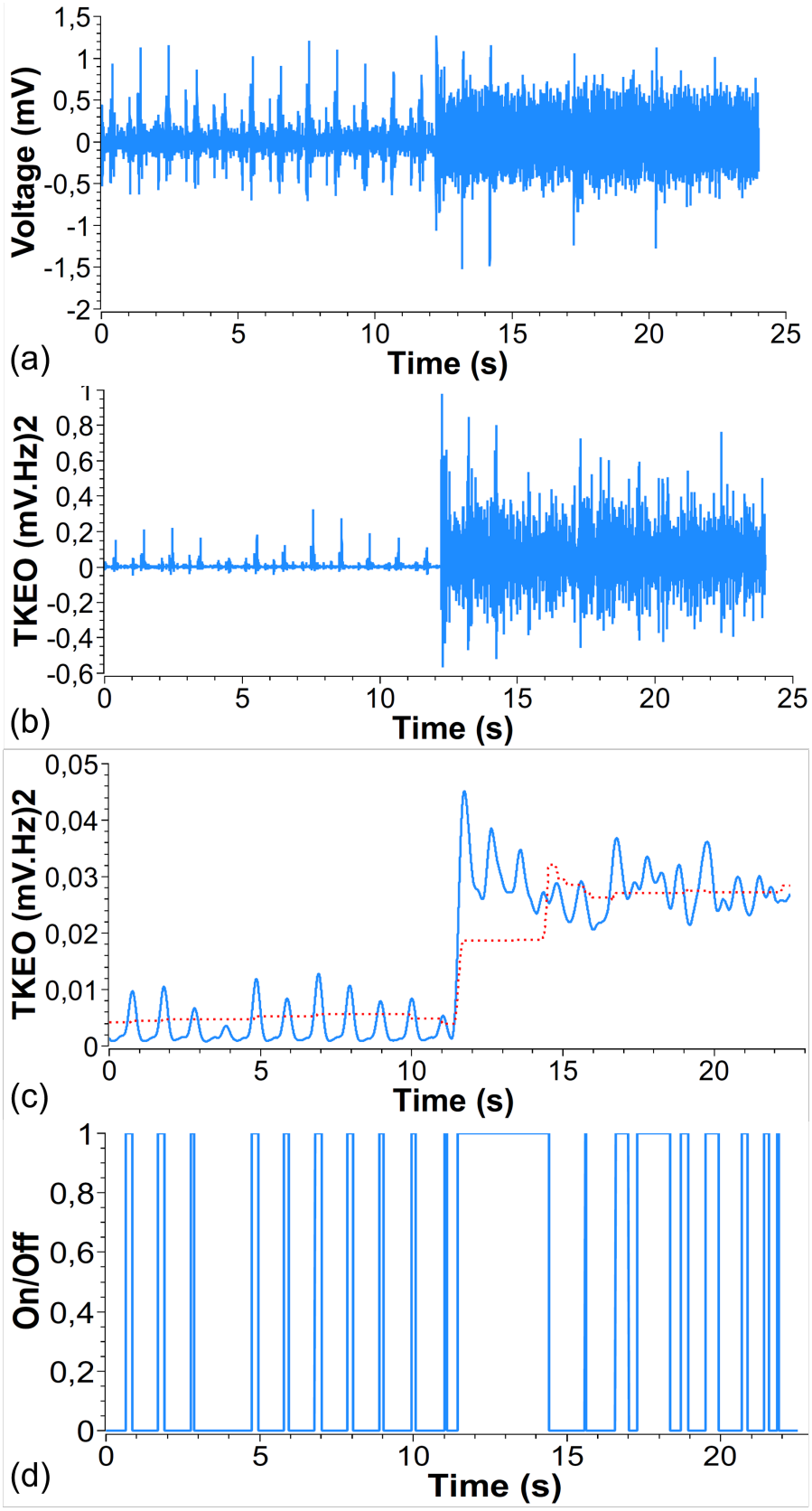

Figure 5.6 (a) A sample from the trials where a sudden change in the noise floor occurs. (b) Signal after the TKEO operator, noise floor is still strongly over there (c) TKEO signal after the median filter, 3 second adaptive threshold is shown with red dash. (d) detected threshold passing.

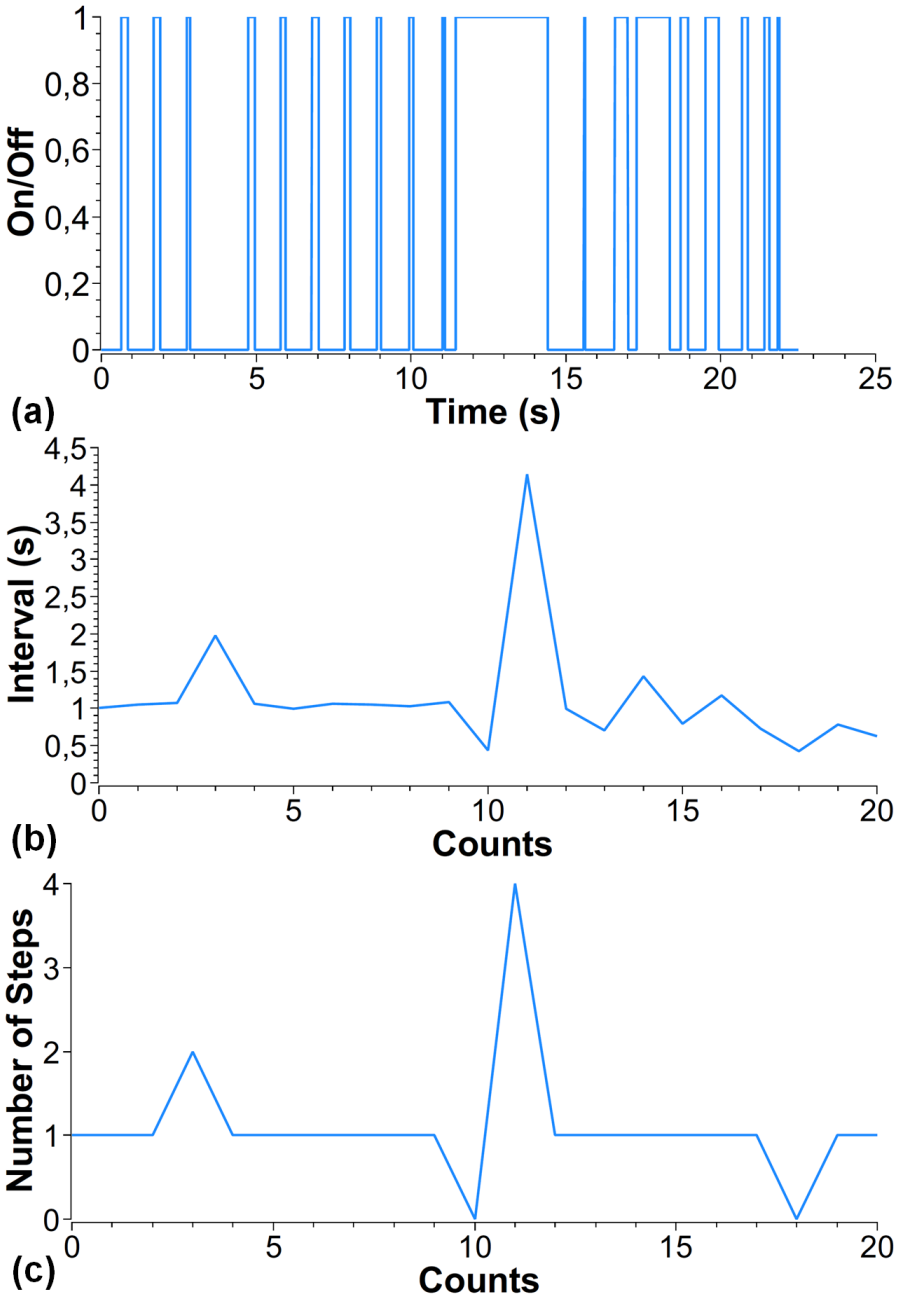

Figure 5.7 (a)Detected steps (b) Time interval of consecutive steps detection for chosen sample signal. Sudden jumps and downs indicate a missed step or false step. (c) Correction of the number of steps. Instead of counting the number of threshold passing instances, algorithm counts the occurrence of the time intervals and calculates the number of steps taken that way.

A comparison of the detected step number with a commercial accelerometer-based pedometer demonstrates the success of the step detection with the graphene textile-based wearable prototype as shown in Table V.1. As expected, increased jogging speed increased the success of the detection since peroneus longus needs to be activated strongly.

Table V.1 Results Of The Threadmill Experiment

Speed (Mil/h)	% of Successful Counts	Standard Deviation
4	89,8457	6,9644574
6	93,2774	7,0657012
8	97,9925	0,4904242

Detected muscle activation patterns could be useful for stand-alone activity tracking or could be used with merging it with an additional accelerometer to provide high accuracy step detection as well as differentiation of non-walking movements [83]. Another possible utilization could be for the pedestrian navigation where the fusion of lower limb EMG data with a compass could be used for stride length and direction detection and compensate for the situations in which satellite navigation systems fail [84].

2 Fatigue Detection

Strong and extended muscle activity would cause a reduction in the contraction capability of that muscle, which is known as localized muscle fatigue [85]. Identifying the muscle fatigue could be useful in various areas such as sport to improve the muscle development of elite athletes or occupational health and ergonomics where muscle load-related injuries could be prevented beforehand [9].

Fig.5.8, summarizes the physiological process of localized muscle fatigue where high muscular load with time would cause accumulation of products, decrease in the energy supply, reduction of membrane excitability and in the end decrease contractability. Studying the muscle biopotentials for fatigue detection appeals to researchers since EMG cues are objective indicators of fatigue compared to subjects' personal comments, and compared to the mechanical indicators, they reveal the fatigue trend earlier. EMG manifestations relate to the change in the median frequency and signal amplitude, whereas mechanical manifestation refers to the loss in force exertion ability [86]. An amplitude increase of the signal during the sustained contraction is due to the recruitment of additional motor units and their growing firing rates to sustain the required force. As the contraction continues, muscle conduction velocity decreases, which shifts the frequency spectrum towards the lower end [86].

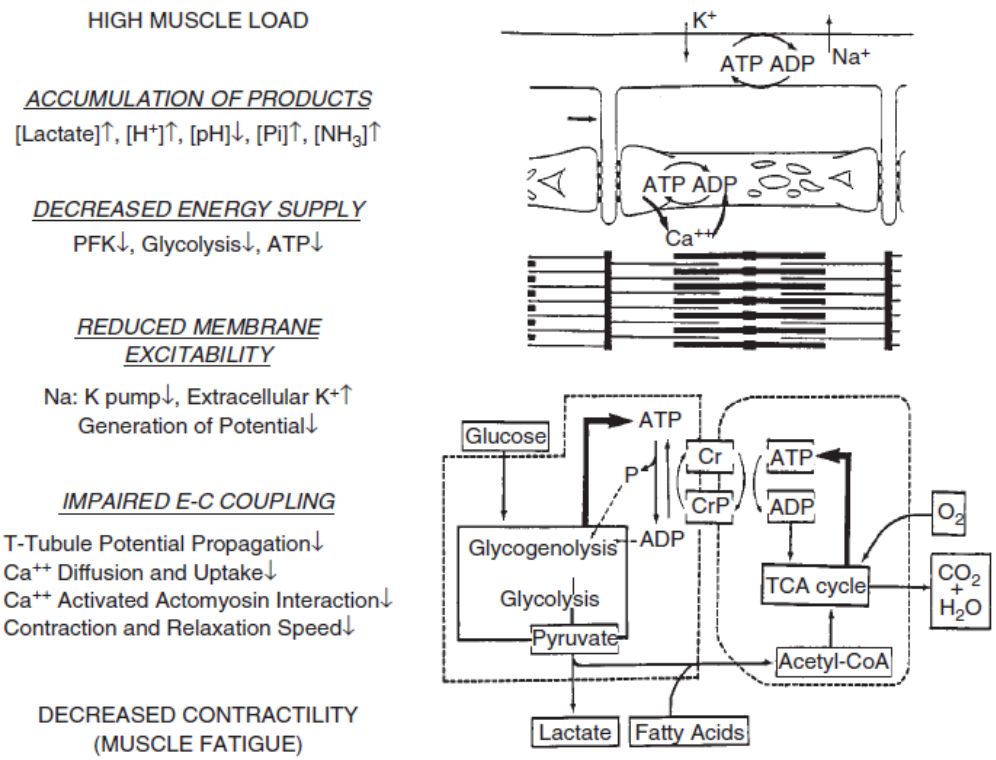

Figure 1.4. Possible metabolic and electrophysiologic consequences of muscular activity that lead to fatigue.

Figure 5.8 Possible metabolic consequences of muscular activity that leads to fatigue [4]

Real time processing of the EMG signals was shown to be a reliable way to harvest fatigue information in dynamic conditions [87, 9]. It was shown that combining the decreasing instantaneous median frequency and increasing signal energy would provide a strong classification indicator called 1D spectro (Fig.5.9)[88].

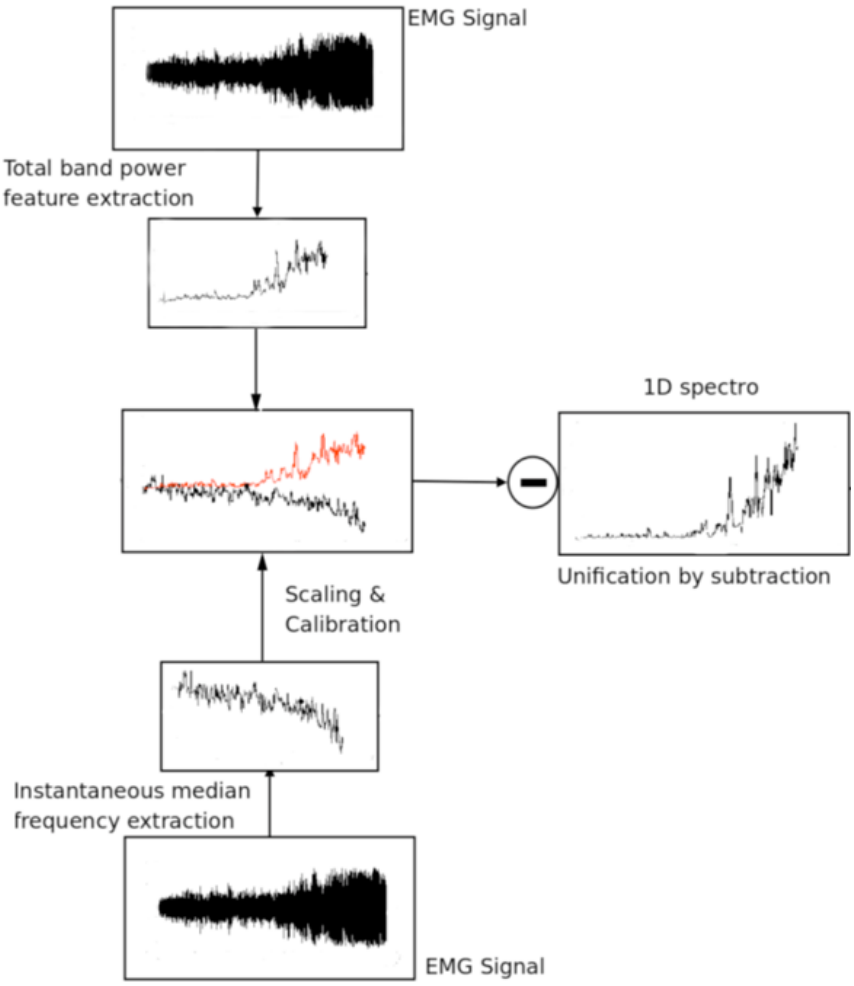

Figure 5.9 Derivation of the 1D spectro [88]

As another example of wearable EMG monitoring, an armband was fabricated to acquire signals coming from biceps brachii (Fig.5.10) and used it for isometric contraction. Conducted exercise displayed smaller background noise thanks to the limited movement and high signal energy level from heavy contractions of the biceps brachii. These ensured an acceptable SNR level, and a corner frequency of the high pass filter was adjusted to be lowered to 20 Hz by changing the related R, C values for more accurate detection of the instantaneous median frequency. For creating a muscle fatigue experiment under isometric contraction, a visual feedback mechanism was designed where the subject was asked to hold a dumbbell of 8 kg in a specific elbow flexion angles until he/she cannot sustain the position. Flexion angle was determined with a mobile phone placed on the subject's wrist, where a goniometer application using the onboard gyroscope of the phone was used to visualize the angular position of the wrist flexion(Fig.5.11). Real time signal processing on the LabVIEW revealed that a clear increase in 1D Spectro exists as the subject

experiences muscle fatigue (Fig.5.12). This trend demonstrates the potential of the developed wearable system with graphene textile electrodes in fatigue detection.

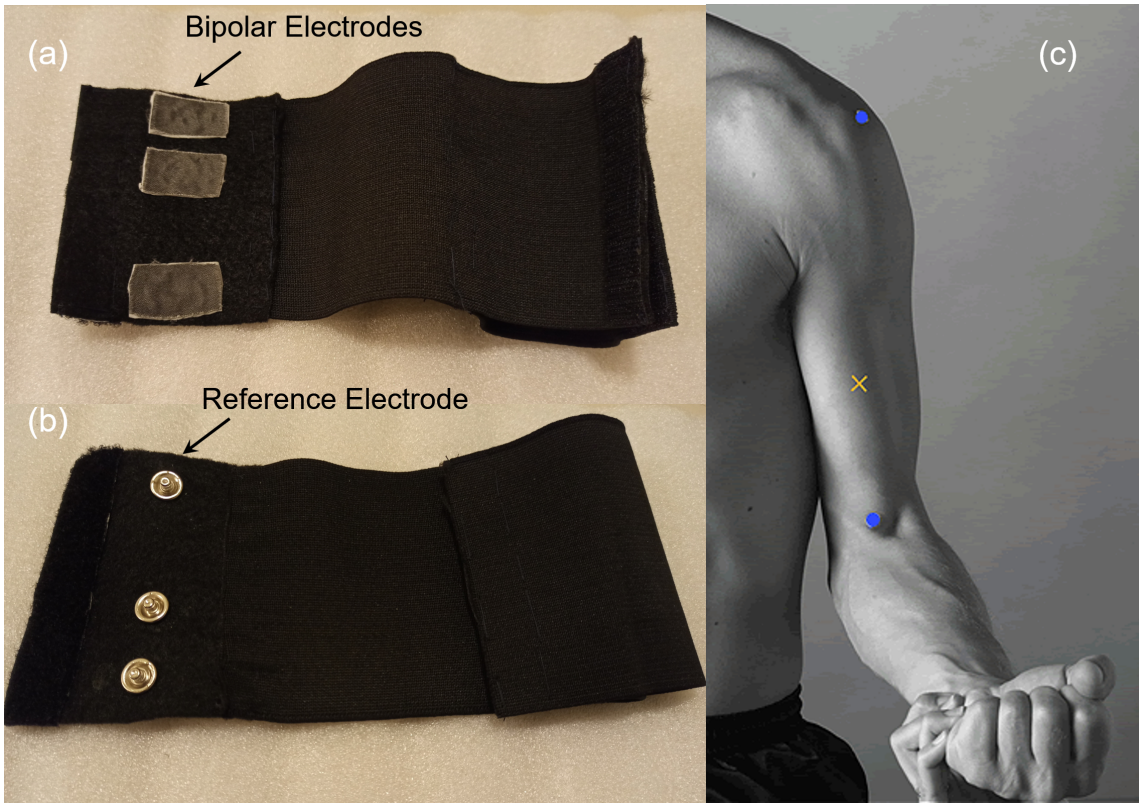

Figure 5.10 Designed arm band (a) inside (b) outside view (c) Position of the biceps brachii indicated with muscle belly and endpoints [78]

Figure 5.11 Experiment setup for the fatigue trial.

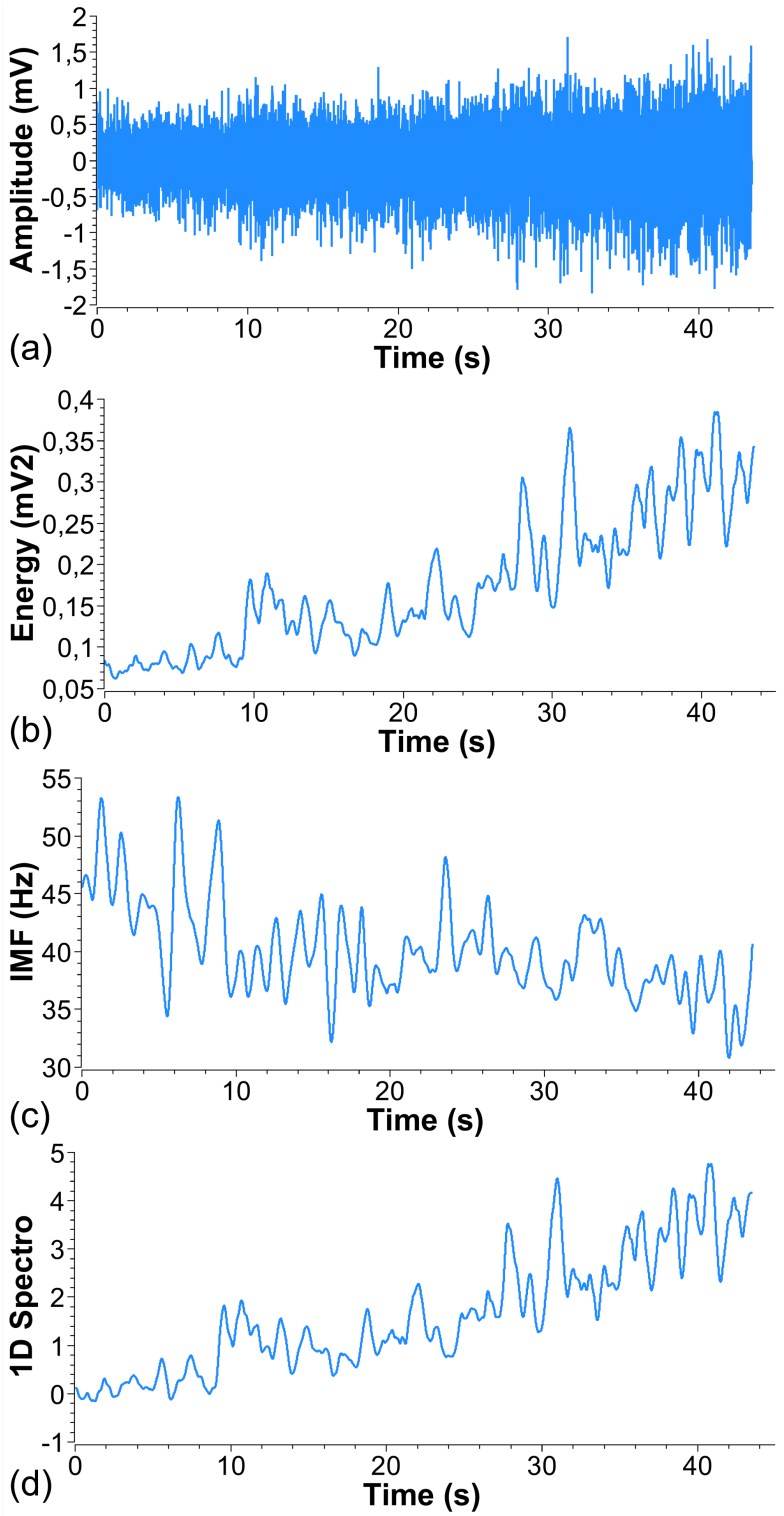

Figure 5.12 A portion of the signal as the subject experiences fatigue (a) Raw signal (b) Spectral energy of the signal (c) Intantenous median frequency (d) 1D spectro.

VI. LONG TERM FUNCTIONALITY

The inability of clinical Ag/AgCl electrodes to cope with long term usability requirements either for single acquisition with extended hours of use or repeated usage for a longer product lifetime was well-documented [89]. These could be summarized shortly as gel-related problems in which electrodes are of single-use by definition, and for extended use scenarios, electrode performance drop due to the drying out of the gel which at the same time causes irritation and discomfort. Long term usability of the textile electrodes, on the other hand, depends on two main factors, which could be stated as biocompatibility and washability. The next two subsections will cover these aspects for graphene textile electrodes.

1 Washability

One of the points that could define the designed wearables' lifespan is about their endurance to washing/cleaning. If conductive textiles easily wear out and lose their conductivity rapidly, then it would be hard to push them to the market for daily life use. Nevertheless, some loss in conductivity expected after a certain number of washing cycles since (probably) absorption of water and mechanical stress loaded on textile fibers during cleaning may decrease or damage the conductive paths [90]. With keeping this in mind, two different washability tests were designed for the produced graphene textile electrodes. One was by using a washing machine to test the durability in the case of extreme mechanical stress, and the other was performed by dipping and keeping the textiles in detergent water without any movement.

For the test with a washing machine, the textile was cleaned in the standard delicate setting, which cleans in 40 degrees at 400 rpm for 30 minutes. After the 5 washing cycles, resistance value increased 2.5 times (Fig 6.1).

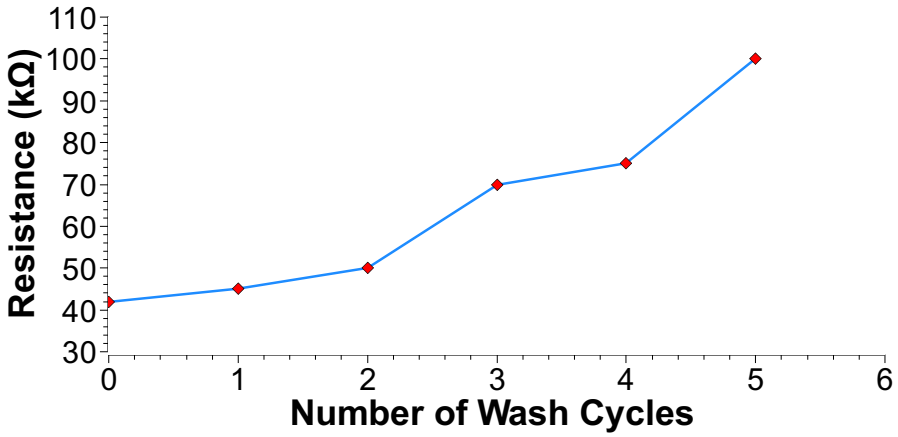

Figure 6.1 Resistance change with wash test over washing machine.

Another conductive textile piece was chosen for a hand wash test, where it was again subjected to 5 washing cycles. Each time textile was dipped into the detergent water, it was kept for 30 minutes, rinsed with clean water, and resistance change was recorded (Fig.6.2). Resistance values increased from 45k to nearly 65k showing less than 50% variation in 5 washing cycles. A comparison of two tests shows that mechanical stress introduced by the washing machine has a negative effect on the resistance values, and hand wash should be preferred to preserve the conductivity of the textiles better.

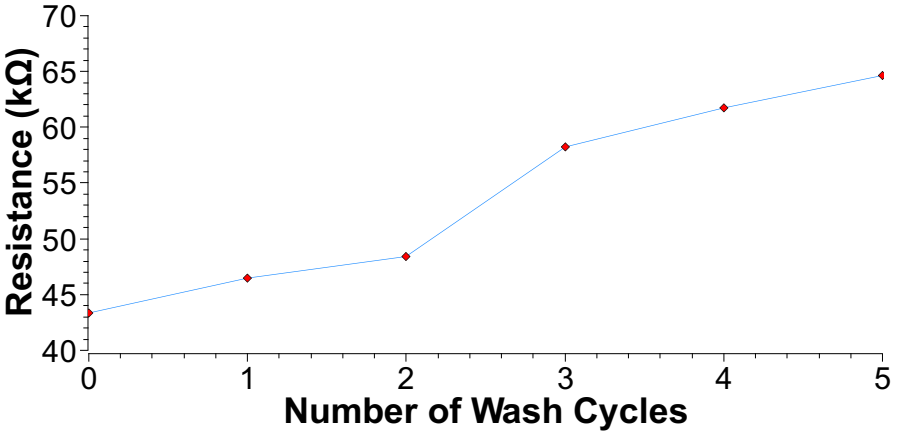

Figure 6.2 Resistance change with hand wash test.

2 Biocompatibility

Another and more fundamental question for long term usage of the textile electrodes is about their biocompatibility. Designed wearables are aimed to be useful for extended hours without removal. In our experiments with EMG wearables, participants have not reported experience of skin irritation. Although it was not possible to clinically test the biocompatibility of the designed textile electrodes, this seemed to be in line with the previous research that concluded graphene cytotoxicity is low for skin contact [91].

VII. CONCLUSIONS

Technological sophistications seem to push us towards the broader use of wearable platforms with biosensing capabilities. Surface EMG of superficial muscles is one of those biosignals that could have wearable applications in a variety of fields. One of the technical challenges on the way of long term wearable EMG acquisition is the integration of comfortable electrodes with desirable performances into garments. Textile electrodes present a natural answer to this problem with their inherent flexibility and breathability; therefore, their study has a central place in wearable EMG acquisition.

This work started with developing conductive graphene textiles and continued with the investigation of their feasibility as textile electrodes and their respective proof-of-concept experiments. System-level design of the wearables included the fabrication of the electroconductive graphene textiles, construction of textile electrodes on an elastic band structure for a specific muscle, design of the battery-powered wireless acquisition unit, implementation of application-specific algorithms and creation of the graphical user interface for the end-user. Two different muscles' (peroneus longus and biceps brachii) sEMG signals were chosen to be home to graphene textile wearables for activity tracking and fatigue indicator applications, respectively. Activity tracking was implemented with counting the muscle activations of peroneus longus muscle and calculating them for voluntary steps. Treadmill experiments were performed with four different subjects for moderate and fast jogging speeds, and results revealed that the designed system could match the step counting with nearly 90% accuracy in the worst-case scenario. Algorithm's ability to adapt the sudden drops in the signal to noise ratio with adaptive thresholding and real time step correcting is important in this regard. This correlation with respect to the step counts that taken only from one channel sEMG shows that a developed system could also be used in sensor fusion, where high accuracy step counting or pedestrian navigation systems could be realized. Examining the muscle fatigue status of biceps brachii in an isometric exercise was the second conducted experiment. A custom fabricated graphene wearable armband was used for this purpose, and it was shown that the

developed system was able to process the sEMG signal for a muscle fatigue classification feature called 1D Spectro. Its correlation with the fatigue experience reported by the experiment subject showed that the developed system could also be improved further for real-time localized muscle fatigue detection, which can be instrumental for a wide variety of topics such as workplace ergonomics, elite athlete training, and rehabilitation.

Moreover, the feasibility of graphene textile electrodes for wearable sEMG acquisition systems was studied in this work. From the electrode performance characterization to signal quality comparisons with clinical electrodes in static exercises graphene textile electrodes were found to be closely following the gold standard electrode performance. Proof of concept graphene electrode embedded wearables was also shown to perform adequately for desired applications. Other than graphene textile electrodes, the practicability of the designed sEMG acquisition wearables was also verified, and they potentially provide a blueprint for the development of similar systems.

BIBLIOGRAPHY

[1] J. Hayward, "Wearable Technology Forecasts 2019-2029." [Online]. Available: https://www.idtechex.com/en/research-report/wearable-technology-forecasts-2019-2029/680

[2] J. Plazak and M. Kersten-Oertel, "A survey on the affordances of "hearables"," *Inventions*, vol. 3, no. 3, p. 48, 2018.

[3] I. Kazani, V. Lutz, S. Malik, A. Mazari, V. Nierstrasz, L. Rodrigues, and S. Tedesco, "Smart textiles for sportswear and wearables (wg5): State-of-the art report. context project," 2020.

[4] R. Merletti and P. Parker, *Electromyography*, R. Merletti and P. Parker, Eds. Hoboken, NJ, USA: John Wiley & Sons, Inc., jul 2004. [Online]. Available: http://doi.wiley.com/10.1002/0471678384

[5] R. Merletti and D. Farina, *Surface Electromyography: Physiology, Engineering and Applications*, 2016.

[6] S. E. Mathiassen, J. Winkel, and G. M. Hägg, "Normalization of surface EMG amplitude from the upper trapezius muscle in ergonomic studies - A review," 1995.

[7] C. Castellini and P. Van Der Smagt, "Surface EMG in advanced hand prosthetics," *Biological Cybernetics*, 2009.

[8] H. Turker and H. Sze, "Surface Electromyography in Sports and Exercise," in *Electrodiagnosis in New Frontiers of Clinical Research*, 2013.

[9] M. R. Al-Mulla, F. Sepulveda, and M. Colley, "An autonomous wearable system for predicting and detecting localised muscle fatigue," *Sensors*, 2011.

[10] O. Tikkanen, M. Hu, T. Vilavuo, P. Tolvanen, S. Cheng, and T. Finni, "Ventilatory threshold during incremental running can be estimated using EMG shorts," *Physiological Measurement*, 2012.

[11] H. Woodford and C. Price, "EMG biofeedback for the recovery of motor function after stroke," 2007.

[12] V. Agostini, A. Nascimbeni, A. Gaffuri, P. Imazio, M. G. Benedetti, and M. Knaflitz, "Normative EMG activation patterns of school-age children during gait," *Gait and Posture*, 2010.

[13] R. Needham and S. J. Davies, "Use of the Grindcare ® device in the management of nocturnal bruxism: A pilot study," *British Dental Journal*, 2013.

[14] M. A. Cavalcanti Garcia and T. M. Vieira, "Surface electromyography: Why, when and how to use it," *Revista Andaluza de Medicina del Deporte*, 2011.

[15] A. J. Golparvar and M. Kaya Yapici, "Wearable graphene textile-enabled EOG sensing," *Proceedings of IEEE Sensors*, vol. 2017-Decem, pp. 1–3, 2017.

[16] A. Shafti, R. B. Ribas Manero, A. M. Borg, K. Althoefer, and M. J. Howard, "Embroidered Electromyography: A Systematic Design Guide," *IEEE Transactions on Neural Systems and Rehabilitation Engineering*, vol. 25, no. 9, pp. 1472–1480, 2017.

[17] C. J. De Luca, "Surface electromyography: Detection and recording," *DelSys Incorporated*, 2002.

[18] G. Acar, "Graphene Textile Smart Clothing for Wearable Cardiac Monitoring," Ph.D. dissertation, Sabanci University, 2019.

[19] H. Y. Song, J. H. Lee, D. Kang, H. Cho, H. S. Cho, J. W. Lee, and Y. J. Lee, "Textile electrodes of jacquard woven fabrics for biosignal measurement," *Journal of the Textile Institute*, 2010.

[20] T. Kannaian, R. Neelaveni, and G. Thilagavathi, "Design and development of embroidered textile electrodes for continuous measurement of electrocardiogram signals," *Journal of Industrial Textiles*, 2013.

[21] N. Karim, S. Afroj, A. Malandraki, S. Butterworth, C. Beach, M. Rigout, K. S. Novoselov, A. J. Casson, and S. G. Yeates, "All inkjet-printed graphene-based conductive patterns for wearable e-textile applications," *Journal of Materials Chemistry C*, vol. 5, no. 44, pp. 11 640–11 648, 2017. [Online]. Available: http://dx.doi.org/10.1039/c7tc03669h

[22] S. H. Lee, S. M. Jung, C. K. Lee, K. S. Jeong, G. Cho, and S. K. Yoo, "Wearable ECG monitoring system using conductive fabrics and active electrodes," in *Lecture Notes in Computer Science (including subseries Lecture Notes in Artificial Intelligence and Lecture Notes in Bioinformatics)*, 2009.

[23] Y. Zhou, X. Ding, J. Zhang, Y. Duan, J. Hu, and X. Yang, "Fabrication of conductive fabric as textile electrode for ECG monitoring," *Fibers and Polymers*, 2014.

[24] M. K. Yapici and T. E. Alkhidir, "Intelligent medical garments with graphene-functionalized smart-cloth ECG sensors," *Sensors (Switzerland)*, 2017.

[25] H. Heidari, S. Zuo, A. Krasoulis, and K. Nazarpour, "CMOS Magnetic Sensors for Wearable Magnetomyography," in *Proceedings of the Annual International Conference of the IEEE Engineering in Medicine and Biology Society, EMBS*, 2018.

[26] R. B. Woodward, M. J. Stokes, S. J. Shefelbine, and R. Vaidyanathan, "Segmenting Mechanomyography Measures of Muscle Activity Phases Using Inertial Data," *Scientific Reports*, 2019.

[27] J. Basmajian and C. DeLuca, *Muscle Alive*. Baltimore: Williams& Wilkins, 1985.

[28] R. F. Kleissen, J. H. Buurke, J. Harlaar, and G. Zilvold, "Electromyography in the biomechanical analysis of human movement and its clinical application," 1998.

[29] G. D. Pope, "Introduction to Surface Electromyography," *Physiotherapy*, 1998.

[30] E. Henneman and L. M. Mendell, "Functional Organization of Motoneuron Pool and its Inputs," in *Comprehensive Physiology*, 2011.

[31] J. A. Stephens and T. P. Usherwood, "The mechanical properties of human motor units with special reference to their fatiguability and recruitment threshold," *Brain Research*, 1977.

[32] R. M. Nelson, T. Cauley, M. Fink, C. Lauretani, and T. Simonson, "Comparison of motor unit action potential characteristics and hand dominance using monopolar needle electrodes in the abductor pollicis brevis and abductor digiti minimi muscles," *Electromyography and Clinical Neurophysiology*, 2003.

[33] H. J. Hermens, B. Freriks, R. Merletti, D. Stegeman, J. Blok, G. Rau, C. Disselhorst-Klug, and G. Hägg, "European Recommendations for Surface ElectroMyoGraphy Results of the SENIAM project," *Roessingh research and development*, 1999.

[34] N. A. Dimitrova, G. V. Dimitrov, and V. N. Chihman, "Effect of electrode dimensions on motor unit potentials," *Medical Engineering and Physics*, 1999.

[35] H. Cheng, Z. Dong, C. Hu, Y. Zhao, Y. Hu, L. Qu, N. Chen, and L. Dai, "Textile electrodes woven by carbon nanotube–graphene hybrid fibers for flexible electrochemical capacitors," *Nanoscale*, vol. 5, no. 8, pp. 3428–3434, 2013.

[36] S. Pan, Z. Yang, P. Chen, J. Deng, H. Li, and H. Peng, "Wearable solar cells by stacking textile electrodes," *Angewandte Chemie*, vol. 126, no. 24, pp. 6224–6228, 2014.

[37] H. Zhou, Y. Lu, W. Chen, Z. Wu, H. Zou, L. Krundel, and G. Li, "Stimulating the comfort of textile electrodes in wearable neuromuscular electrical stimulation," *Sensors*, vol. 15, no. 7, pp. 17 241–17 257, 2015.

[38] M. Stoppa and A. Chiolerio, "Wearable electronics and smart textiles: A critical review," 2014.

[39] H. Qin, J. Li, B. He, J. Sun, L. Li, and L. Qian, "Novel wearable electrodes based on conductive chitosan fabrics and their application in smart garments," *Materials*, 2018.

[40] A. Alzaidi, L. Zhang, and H. Bajwa, "Smart textiles based wireless ECG system," in *2012 IEEE Long Island Systems, Applications and Technology Conference, LISAT 2012*, 2012.

[41] G. Cho, K. Jeong, M. J. Paik, Y. Kwun, and M. Sung, "Performance evaluation of textile-based electrodes and motion sensors for smart clothing," *IEEE Sensors Journal*, 2011.

[42] M. K. Yapici, T. Alkhidir, Y. A. Samad, and K. Liao, "Graphene-clad textile electrodes for electrocardiogram monitoring," *Sensors and Actuators, B: Chemical*, 2015.

[43] S. Takamatsu, T. Lonjaret, D. Crisp, J. M. Badier, G. G. Malliaras, and E. Ismailova, "Direct patterning of organic conductors on knitted textiles for long-term electrocardiography," *Scientific Reports*, 2015.

[44] G. Acar, O. Ozturk, A. J. Golparvar, T. A. Elboshra, K. Böhringer, and M. Kaya Yapici, "Wearable and flexible textile electrodes for biopotential signal monitoring: A review," *Electronics (Switzerland)*, 2019.

[45] S. Lee, Y. Lee, J. Park, and D. Choi, "Stitchable organic photovoltaic cells with textile electrodes," *Nano Energy*, 2014.

[46] T. Pola and J. Vanhala, "Textile electrodes in ECG measurement," in *Proceedings of the 2007 International Conference on Intelligent Sensors, Sensor Networks and Information Processing, ISSNIP*, 2007.

[47] S. Jang, J. Cho, K. Jeong, and G. Cho, "Exploring possibilities of ECG electrodes for bio-monitoring smartwear with Cu sputtered fabrics," in *Lecture Notes in Computer Science (including subseries Lecture Notes in Artificial Intelligence and Lecture Notes in Bioinformatics)*, 2007.

[48] B. Taji, S. Shirmohammadi, V. Groza, and I. Batkin, "Impact of skin-electrode interface on electrocardiogram measurements using conductive textile electrodes," *IEEE Transactions on Instrumentation and Measurement*, 2014.

[49] J. Webster, "Medical instrumentation: application and design, Fourth edition." *John Wiley and Sons, Inc. USA*, 2010.

[50] L. Xie, G. Yang, L. Xu, F. Seoane, Q. Chen, and L. Zheng, "Characterization of dry biopotential electrodes," in *Proceedings of the Annual International Conference of the IEEE Engineering in Medicine and Biology Society, EMBS*, 2013.

[51] A. Baba and M. Burke, "Electrical characterisation of dry electrodes for ECG recording," *WSEAS International Conference*, 2008.

[52] E. P. Scilingo, A. Gemignani, R. Paradiso, N. Taccini, B. Ghelarducci, and D. De Rossi, "Performance evaluation of sensing fabrics for monitoring physiological and biomechanical variables," *IEEE Transactions on Information Technology in Biomedicine*, 2005.

[53] W. Wu, S. Pirbhulal, A. K. Sangaiah, S. C. Mukhopadhyay, and G. Li, "Optimization of signal quality over comfortability of textile electrodes for ECG monitoring in fog computing based medical applications," *Future Generation Computer Systems*, 2018.

[54] G. Paul, R. Torah, S. Beeby, and J. Tudor, "The development of screen printed conductive networks on textiles for biopotential monitoring applications," *Sensors and Actuators, A: Physical*, 2014.

[55] G. Priniotakis, P. Westbroek, L. Van Langenhove, and C. Hertleer, "Electrochemical impedance spectroscopy as an objective method for characterization of textile electrodes," *Transactions of the Institute of Measurement & Control*, 2007.

[56] J. G. Webster, "Reducing Motion Artifacts and Interference in Biopotential Recording," *IEEE Transactions on Biomedical Engineering*, 1984.

[57] A. Cömert and J. Hyttinen, "Investigating the possible effect of electrode support structure on motion artifact in wearable bioelectric signal monitoring," *BioMedical Engineering Online*, 2015.

[58] E. J. Pino, Y. Arias, and P. Aqueveque, "Wearable EMG Shirt for Upper Limb Training," in *Proceedings of the Annual International Conference of the IEEE Engineering in Medicine and Biology Society, EMBS*, 2018.

[59] B. Sumner, C. Mancuso, and R. Paradiso, "Performances evaluation of textile electrodes for EMG remote measurements," in *Proceedings of the Annual International Conference of the IEEE Engineering in Medicine and Biology Society, EMBS*, 2013.

[60] A. Niijima, T. Yamada, T. Isezaki, R. Aoki, and T. Watanabe, "HitoeCap: Wearable EMG sensor for monitoring masticatory muscles with PEDOT-PSS textile electrodes," in *Proceedings - International Symposium on Wearable Computers, ISWC*, 2017.

[61] D. Farina, T. Lorrain, F. Negro, and N. Jiang, "High-density EMG E-textile systems for the control of active prostheses," in *2010 Annual International Conference of the IEEE Engineering in Medicine and Biology Society, EMBC'10*, 2010.

[62] G. Li, Y. Geng, D. Tao, and P. Zhou, "Performance of electromyography recorded using textile electrodes in classifying arm movements," in *Proceedings of the Annual International Conference of the IEEE Engineering in Medicine and Biology Society, EMBS*, 2011.

[63] J. Guo, S. Yu, Y. Li, T. H. Huang, J. Wang, B. Lynn, J. Fidock, C. L. Shen, D. Edwards, and H. Su, "A soft robotic exo-sheath using fabric EMG sensing for hand rehabilitation and assistance," in *2018 IEEE International Conference on Soft Robotics, RoboSoft 2018*, 2018.

[64] O. Tikkanen, S. Kärkkäinen, P. Haakana, M. Kallinen, T. Pullinen, and T. Finni, "EMG, heart rate, and accelerometer as estimators of energy expenditure in locomotion," *Medicine and Science in Sports and Exercise*, 2014.

[65] R. Zhang, S. Bernhart, and O. Amft, "Diet eyeglasses: Recognising food chewing using EMG and smart eyeglasses," in *BSN 2016 - 13th Annual Body Sensor Networks Conference*, 2016.

[66] A. J. Golparvar and M. K. Yapici, "Graphene smart textile-based wearable eye movement sensor for electro-ocular control and interaction with objects," *Journal of The Electrochemical Society*, vol. 166, no. 9, p. B3184, 2019.

[67] M. Shateri-Khalilabad and M. E. Yazdanshenas, "Fabricating electroconductive cotton textiles using graphene," *Carbohydrate Polymers*, 2013.

[68] S. Grimnes, "Impedance measurement of individual skin surface electrodes," *Medical & Biological Engineering & Computing*, 1983.

[69] P. Konrad, "The ABC of EMG A Practical Introduction to Kinesiological Electromyography," *Noraxon INC. USA. A*, 2005.

[70] Y. G. Lim, K. K. Kim, and K. S. Park, "ECG measurement on a chair without conductive contact," *IEEE Transactions on Biomedical Engineering*, 2006.

[71] A. J. Golparvar, "Graphene-coated wearable textiles for EOG-based human-computer interaction Biopotential Measurement using Graphene-based Textile Electrodes View project," no. April, 2018. [Online]. Available: https://www.researchgate.net/publication/324252426

[72] A. Cömert, M. Honkala, and J. Hyttinen, "Effect of pressure and padding on motion artifact of textile electrodes," *BioMedical Engineering Online*, 2013.

[73] V. Agostini and M. Knaflitz, "An algorithm for the estimation of the signal-to-noise ratio in surface myoelectric signals generated during cyclic movements," *IEEE Transactions on Biomedical Engineering*, 2012.

[74] B. B. Winter and B. B. Winter, "Driven-Right-Leg Circuit Design," *IEEE Transactions on Biomedical Engineering*, 1983.

[75] A. J. Golparvar and M. K. Yapici, "Graphene textiles toward wearable eye tracking sensory system for human-machine interaction in assistive technologies." submitted.

[76] K. J. Brickwood, G. Watson, J. O'Brien, and A. D. Williams, "Consumer-based wearable activity trackers increase physical activity participation: Systematic review and meta-analysis," 2019.

[77] R. Bavdek, A. Zdolšek, V. Strojnik, and A. Dolenec, "Peroneal muscle activity during different types of walking," *Journal of Foot and Ankle Research*, 2018.

[78] SENIAM, "Recommendations for sensor locations in arm or hand muscles," 2015.

[79] S. Solnik, P. Rider, K. Steinweg, P. Devita, and T. Hortobágyi, "Teager-Kaiser energy operator signal conditioning improves EMG onset detection," *European Journal of Applied Physiology*, 2010.

[80] J. F. Kaiser, "On a simple algorithm to calculate the 'energy' of a signal," in *ICASSP, IEEE International Conference on Acoustics, Speech and Signal Processing - Proceedings*, 1990.

[81] S. Mukhopadhyay and G. C. Ray, "A new interpretation of nonlinear energy operator and its efficacy in spike detection," 1998.

[82] X. Li and A. S. Aruin, "Muscle activity onset time detection using Teager-Kaiser energy operator," in *Annual International Conference of the IEEE Engineering in Medicine and Biology - Proceedings*, 2005.

[83] P. Farago, R. Groza, and S. Hintea, "High precision activity tracker based on the correlation of accelerometer and EMG data," in *2019 42nd International Conference on Telecommunications and Signal Processing, TSP 2019*, 2019.

[84] R. Chen, W. Chen, X. Chen, X. Zhang, and Y. Chen, "Sensing strides using EMG signal for pedestrian navigation," *GPS Solutions*, 2011.

[85] D. B. Chaffin, "Localized muscle fatigue — Definition and measurement," *Journal of Occupational Medicine*, 1973.

[86] M. Asghari Oskoei, H. Hu, and J. Q. Gan, "Manifestation of fatigue in myoelectric signals of dynamic contractions produced during playing PC games." *Conference proceedings : ... Annual International Conference of the IEEE Engineering in Medicine and Biology Society. IEEE Engineering in Medicine and Biology Society. Conference*, 2008.

[87] M. S. Hussain and M. Mamun, "Effectiveness of the wavelet transform on the surface EMG to understand the muscle fatigue during walk," 2012.

[88] M. R. Al-Mulla and F. Sepulveda, "A novel feature assisting in the prediction of semg muscle fatigue towards a wearable autonomous system," in *Proceedings of the 2010 IEEE 16th International Mixed-Signals, Sensors and Systems Test Workshop, IMS3TW 2010*, 2010.

[89] N. Meziane, J. G. Webster, M. Attari, and A. J. Nimunkar, "Dry electrodes for electrocardiography," *Physiological Measurement*, 2013.

[90] A. Ankhili, X. Tao, C. Cochrane, D. Coulon, and V. Koncar, "Washable and reliable textile electrodes embedded into underwear fabric for electrocardiography (ECG) monitoring," *Materials*, 2018.

[91] M. Pelin, L. Fusco, V. León, C. Martín, A. Criado, S. Sosa, E. Vázquez, A. Tubaro, and M. Prato, "Differential cytotoxic effects of graphene and graphene oxide on skin keratinocytes," *Scientific Reports*, 2017.